Biologically Useful Chelators That Take Up Ca^{2+} upon Illumination†

S. R. Adams,‡ J. P. Y. Kao,‡ and R. Y. Tsien*,‡

Contribution from the Department of Physiology-Anatomy, University of California, Berkeley, California 94720. *Received April 14, 1989*

Abstract: Two approaches were explored toward the goal of synthesizing physiologically useful Ca^{2+}-selective chelators whose Ca^{2+} affinities increase markedly upon photolysis. In the first approach, the known Ca^{2+}-selective chelator 1,2-bis(*o*-aminophenoxy)ethane-*N*,*N*,*N*′,*N*′-tetraacetic acid (BAPTA) was masked with a variety of photoremovable protecting groups on one of its four carboxyl groups, reducing its affinity for Ca^{2+} to $\sim 10^5$ M^{-1}. Upon irradiation around 365 nm, free chelator with an affinity constant $\sim 10^7$ M^{-1} was regenerated but with very low quantum efficiencies (≤ 0.007). A more successful approach was to manipulate one of the coordinating nitrogens by remote inductive effects. Addition of an electron-withdrawing diazoacetyl substituent to one ring of BAPTA, para to the amino group, resulted in "diazo-2", a chelator with a Ca^{2+} affinity of 4.5×10^5 M^{-1}. Photochemical rearrangement of the diazoacetyl group converted it into an electron-donating carboxymethyl group, causing the Ca^{2+} affinity to increase 30-fold to 1.4×10^7 M^{-1}. The photolysis of Ca^{2+}-free diazo-2 had a quantum efficiency with 365-nm light (λ_{max} 370 nm, $\epsilon \sim 22000$ M^{-1} cm^{-1}) of ~ 0.03 and generated the high-affinity chelator with rate constants of 2300 s^{-1} after a flash. Ca^{2+} was then bound with association and dissociation rate constants of 8.0×10^8 M^{-1} s^{-1} and 58 s^{-1}, respectively. Diazo-2 was incorporated into rat fibroblasts either by microinjection or by incubation as the membrane-permeable, enzymatically labile tetrakis(acetoxymethyl) ester and, when flash-photolyzed, caused a drop in intracellular free $[Ca^{2+}]$ to or below resting values of $\sim 10^{-7}$ M. An even larger increase in affinity (1600-fold) was obtained by substituting both phenyl rings of BAPTA with diazoacetyl substituents. Therefore, these chelators can be used to generate controlled fast decrements in intracellular free $[Ca^{2+}]$ to mimic or ablate a host of important cellular responses, especially in nerve and muscle.

The recent introduction of photosensitive derivatives of nucleotides,[1] inositol polyphosphates,[2] neurotransmitters,[3] calcium,[4] and protons,[5] which release the physiologically active compound with a light flash, has enabled the dynamics of biological responses to be probed noninvasively within cells on a microsecond to millisecond time scale.[6] Our group has concentrated on the photochemical manipulation of intracellular free Ca^{2+} concentration ($[Ca^{2+}]_i$) with the introduction of the "nitr" series of chelators, which release Ca^{2+} upon illumination with long-wavelength UV light.[4a,b] Thus, when loaded into cells either through microinjection or through incubation with the membrane-permeant acetoxymethyl ester, the nitr compounds can be irradiated to generate spikes or plateaus of elevated $[Ca^{2+}]_i$. Nitr-5 has been used in cultured rat sympathetic neutrons to study the activation stoichiometry and kinetics of the Ca^{2+}-activated K^+-conducting channel,[7] and in skeletal muscle to examine the kinetics of Ca^{2+} regulation of troponin C.[8] In conjunction with fluo-3, a fluorescent Ca^{2+} indicator[9] that is excited at longer wavelengths than nitr-5, the $[Ca^{2+}]_i$ can be monitored during photolysis and has been used to examine the temporal role of Ca^{2+} in oscillations of $[Ca^{2+}]_i$ in rat embryo fibroblasts.[10]

We report here the design, synthesis, characterization, and biological application of a series of chelators whose Ca^{2+} affinity is increased upon photolysis, an effect opposite to that exhibited by the nitr series of photolabile Ca^{2+} chelators. Therefore, these chelators could prevent or truncate a rise in $[Ca^{2+}]$. This new series of chelators, like the nitr series, is based on the parent Ca^{2+} chelator, BAPTA, and retains its high selectivity for Ca^{2+} over Mg^{2+}, its insensitivity to pH variations above pH 7, and its fast Ca^{2+} binding kinetics.[11]

The ideal "caged" Ca^{2+} chelator should fulfill the following requirements: (1) The initial Ca^{2+} affinity of the chelator before photolysis should be as weak as possible but certainly with dissociation constant $K_d > 10^{-6}$ M; (2) after photochemical con-

Scheme I

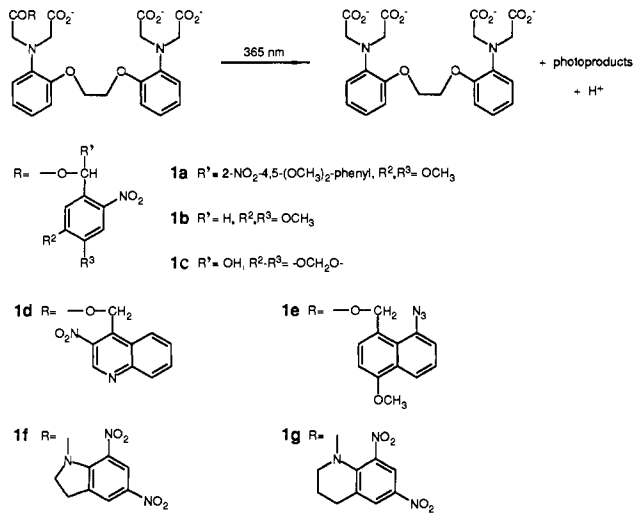

† BAPTA, 1,2-bis(*o*-aminophenoxy)ethane-*N*,*N*,*N*′,*N*′-tetraacetic acid; BDNPM, bis(4,5-dimethoxy-2-nitrophenyl)methyl; $[Ca^{2+}]_i$, cytosolic free Ca^{2+} concentration; diazo-2/AM, the tetrakis(acetoxymethyl) ester of diazo-2; diazo-3/AM, the bis(acetoxymethyl) ester of diazo-3; DMF, *N*,*N*-dimethylformamide; EGTA, ethylenebis(oxyethylenenitrilo)tetraacetic acid, or ethylene glycol bis(2-aminoethyl ether)-*N*,*N*,*N*′,*N*′-tetraacetic acid; fluo-3/AM, the pentakis(acetoxymethyl) ester of fluo-3; HEEDTA, *N*-(2-hydroxyethyl)-ethylenediamine-*N*,*N*′,*N*′-triacetic acid; HEPES, *N*-(2-hydroxyethyl)-piperazine-*N*′-2-ethanesulfonic acid; MOPS, 3-morpholinopropanesulfonic acid; RPTLC, reverse-phase thin-layer chromatography; Tris, tris(hydroxymethyl)aminomethane.

‡ Current address: Department of Pharmacology M-036, School of Medicine, University of California—San Diego, La Jolla, CA 92093.

(1) (a) Kaplan, J. H.; Forbush, B.; Hoffman, J. R. *Biochemistry* **1978**, *17*, 1929-1935. (b) McCray, J. A.; Herbette, L.; Kihara, T.; Trentham, D. R. *Proc. Natl. Acad. Sci. U.S.A.* **1980**, *77*, 7237-7241. (c) Nerbonne, J. M.; Richard, S.; Nargeot, J.; Lester, H. A. *Nature (London)* **1984**, *310*, 74-76. (d) Walker, J. W.; Reid, G. P.; McCray, J. A.; Trentham, D. R. *J. Am. Chem. Soc.* **1988**, *110*, 7170-7177.

(2) Walker, J. W.; Somlyo, A. V.; Goldman, Y. E.; Somlyo, A. P.; Trentham, D. R. *Nature (London)* **1987**, *327*, 249-252.

(3) Walker, J. W.; McCray, J. A.; Hess, G. P. *Biochemistry* **1986**, *25*, 1799-1805.

(4) (a) Tsien, R. Y.; Zucker, R. S. *Biophys. J.* **1986**, *50*, 843-853. (b) Adams, S. R.; Kao, J. P. Y.; Grynkiewicz, G.; Minta, A.; Tsien, R. Y. *J. Am. Chem. Soc.* **1988**, *110*, 3212-3220. (c) Ellis-Davies, G. C. R.; Kaplan, J. H. *J. Org. Chem.* **1988**, *53*, 1966-1969. (d) Kaplan, J. H.; Ellis-Davies, G. C. R. *Proc. Natl. Acad. Sci. U.S.A.* **1988**, *85*, 6571-6575.

(5) McCray, J. A.; Trentham, D. R. *Biophys. J.* **1985**, *47*, 406a.

(6) Gurney, A. M.; Lester, H. A. *Physiol. Rev.* **1987**, *67*, 583-617.

(7) Gurney, A. M.; Tsien, R. Y., Lester, H. A. *Proc. Natl. Acad. Sci. U.S.A.* **1987**, *84*, 3496-3500.

(8) Ashley, C. C.; Barsotti, R. J.; Ferenczi, M. A.; Lea, T. J.; Mulligan, I. P.; Tsien, R. Y. *J. Physiol. (London)* **1987**, *390*, 144P.

(9) (a) Minta, A.; Kao, J. P. Y.; Tsien, R. Y. *J. Biol. Chem.* **1989**, *264*, 8171-8178. (b) Kao, J. P. Y., Harootunian, A. T.; Tsien, R. Y. *J. Biol. Chem.* **1989**, *264*, 8179-8184.

0002-7863/89/1511-7957$01.50/0

Table I[a]

chelator	λ_{max}, nm ($\epsilon_{max} \times 10^{-3}$, M^{-1} cm^{-1})[b] free	λ_{max}, nm ($\epsilon_{max} \times 10^{-3}$, M^{-1} cm^{-1})[b] +Ca^{2+}	$K_d(Ca^{2+})$,[c] μM before	$K_d(Ca^{2+})$,[c] μM after	$K_d(Mg^{2+})$,[d] mM before	$K_d(Mg^{2+})$,[d] mM after	Φ[e] free	Φ[e] +Ca^{2+}	photolysis yield,[f] %	τ,[g] μs free	τ,[g] μs +Ca^{2+}
BDNPM-	346 (7.6)	346 (7.6)	~50	0.16	*h*	*h*	0.0071	0.0071	*h*	*h*	*h*
BAPTA (**1a**)	289 (11)	274 (9)									
1b	345 (5)	345 (5)	*h*	*h*	*h*	*h*	<0.001	<0.001	*h*	*h*	*h*
1c	360 (4.1)	360 (4.1)	*h*	*h*	*h*	*h*	<0.001	<0.001	*h*	*h*	*h*
1d	365sh (1.1)	365sh (1.1)	*h*	*h*	*h*	*h*	<0.001	<0.001	*h*	*h*	*h*
1e	315 (6.5)	315 (6.3)	0.550	∞	*h*	*h*	~1	~1	*h*	*h*	*h*
1f	350 (8.0)	338 (7.8)	*h*	*h*	*h*	*h*	<0.001	~0.01	*h*	*h*	*h*
1g	340 (6.5)	335 (5.0)	*h*	*h*	*h*	*h*	<0.001	~0.05	*h*	*h*	*h*
diazo-1A (**2a**)	365 (16.3)	374 (4.6) 324 (5.8)	176	~300	>100	>100	0.82	>0.9	0	*h*	*h*
diazo-1B (**2b**)	500 (0.3) 350 (2.5) 298 (4.1)	500 (0.3) 350 (2.5) 284 (3.4)	0.15	*h*	*h*	*h*	*h*	*h*	0	*h*	*h*
diazo-2 (**3a**)	370 (22.2)	320 (20.2)	2.2	0.073 0.15[i]	5.5	3.4	0.030	0.057	90	433 ± 44[j]	134 ± 12[j]
diazo-3 (**4a**)	374 (22.8)	*h*	*h*	*h*	*h*	~20	0.048	*h*	0	239 ± 19[j]	*h*
diazo-4 (**5a**)	371 (46.0)	320 (42.3)	89	0.055	*h*	2.6	0.015[k]	0.015[k]	80	*h*	*h*

[a] All measurements were made at 0.1–0.15 M ionic strength, pH 7.0–7.4, and 20–23 °C except where noted (see the Experimental Section and Figures 1 and 2 for details). [b] Absorption maxima and corresponding extinction coefficients (in parentheses) of the dominant peaks at longest wavelength. [c] Dissociation constant for Ca^{2+}, i.e., $K_d(Ca^{2+}) = [Ca^{2+}][\text{free chelator}]/[Ca^{2+}\text{-complex}]$, before and after photolysis. [d] Dissociation constant for Mg^{2+}, i.e., $K_d(Mg^{2+}) = [Mg^{2+}][\text{free chelator}]/[Mg^{2+}\text{-complex}]$, before and after photolysis. [e] Quantum efficiency of photolysis at zero or saturating $[Ca^{2+}]$. [f] Yield of high-affinity Ca^{2+} chelator after photolysis. [g] Time constant or reciprocal rate constant for main component of absorbance decrease of cresol red, attributed to formation of phenylacetates and H^+ release after flash photolysis in zero or saturating $[Ca^{2+}]$. [h] Not determined. [i] Measurement made at 0.25 M ionic strength (0.2 M KCl, 0.05 M NaCl) at 18 °C. [j] An additional fast alkalinization component was present whose rate could not be determined accurately. [k] Quantum efficiency for photolysis of both diazoketone substituents.

Scheme II

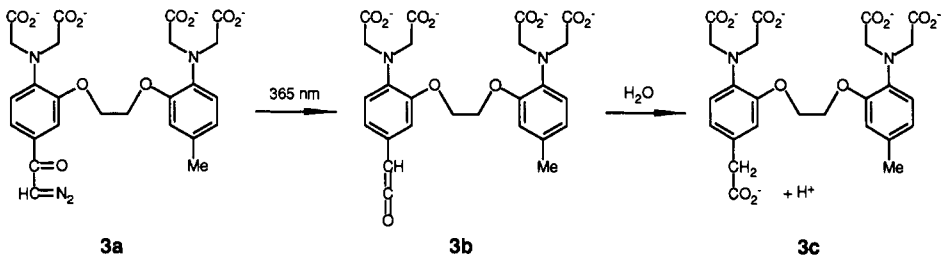

3a **3b** **3c**

version, the chelator K_d should be at or below 10^{-7} M to match the resting $[Ca^{2+}]_i$ found in nearly all cells; (3) the photochemistry and Ca^{2+} uptake should be complete in $\leq 10^{-3}$ s; (4) the wavelength and intensity of the light required for photolysis should not significantly perturb the cells; and (5) the photochemistry should not generate toxic byproducts or other biologically active substances.

Our first attempts were to esterify one of the carboxyl groups of BAPTA with a photosensitive protecting group, thereby increasing the dissociation constant for Ca^{2+} to $\sim 10^{-4}$ M. Photolysis would release BAPTA, whose Ca^{2+} affinity would be sufficient to bind significant amounts of Ca^{2+} at resting $[Ca^{2+}]_i$ (Scheme I, Table I). However, none of the known photoremovable carboxyl protecting groups proved sufficiently effective. Our second approach was to exploit the ease of adjusting the Ca^{2+} affinity of BAPTA by suitable substitution on its benzene rings.[11] These new chelators, the diazo series, incorporate an electron-withdrawing diazoacetyl group, which on photolysis undergoes the Wolff rearrangement via the ketene to give the electron-donating carboxymethyl substituent (Scheme II, Table I). Thereby, a chelator with initially low affinity for Ca^{2+} is photochemically converted to one with high affinity without steric modification of the metal binding site.

Results

Photochemical and Synthetic Strategy. Our first efforts were directed toward finding a suitable photoremovable protecting group[12] for carboxylic acids that could be used in aqueous solution and that absorbed at wavelengths longer than 350 nm. 2-Nitrobenzyl esters[13] and (2-nitrophenyl)amino[14] derivatives have been used successfully in peptide synthesis;[12] however, little information about quantum yields of photoconversion has been reported.[15] Therefore, as a model system, derivatives of acetic acid were synthesized and photolyzed under part-aqueous conditions. The quantum yield was measured by loss of starting material following separation by HPLC (Table II). To improve the extinction coefficient of the 2-nitrobenzyl group at >350 nm, two methoxy groups were added to give the 2-nitro-4,5-dimethoxybenzyl group; however, this drastically decreased the quantum yield compared to the free alcohol or methyl ether. By addition of another dimethoxy-2-nitrophenyl group at the α position [to give the bis(4,5-dimethoxy-2-nitrophenyl)methyl derivative][13b] the quantum yield was improved 5-fold but was still low. More photosensitive derivatives of 2-nitrobenzyl esters that incorporated an α-nitrile or ester group or replaced the benzene with a quinoline showed a dark reaction lasting tens of minutes (data not shown). The (*o*-nitrophenyl)amino group as a photoremovable carboxyl protecting group was introduced by Patchornik and co-workers.[14]

(10) Harootunian, A. T.; Kao, J. P. Y.; Tsien, R. Y. *Cold Spring Harbor Symp. Quant. Biol.* **1988**, *53*, 935–943.
(11) Tsien, R. Y. *Biochemistry* **1980**, *19*, 2396–2404.
(12) (a) Binkley, R. W.; Flechtner, T. W. In *Synthetic Organic Photochemistry*; Horspool, W. M., Ed.; Plenum: New York, 1984; pp 375–423. (b) Pillai, V. N. R. *Org. Photochem.* **1987**, *9*, 225–323.
(13) (a) Barltrop, J. A.; Plant, P. J.; Schofield, P. *J. Chem. Soc., Chem. Commun.* **1966**, 822–823. (b) Patchornik, A.; Amit, B.; Woodward, R. B. *J. Am. Chem. Soc.* **1970**, *92*, 6333–6335.
(14) (a) Amit, B.; Patchornik, A. *Tetrahedron Lett.* **1973**, 2205–2208. (b) Amit, B.; Ben-Efraim, D. A.; Patchornik, A. *J. Am. Chem. Soc.* **1976**, *98*, 843–844. (c) Amit, B.; Ben-Efraim, D. A.; Patchornik, A. *J. Chem. Soc., Perkin Trans. 1* **1976**, 57–63.
(15) (a) Schupp, H.; Wong, W. K.; Schnabel, W. *J. Photochem.* **1987**, *36*, 85–97. (b) Zhu, Q. Q.; Schnabel, W.; Schupp, H. *J. Photochem.* **1987**, *39*, 317–322.

Table II. Quantum Yields for 2-Nitrobenzyl and (2-Nitrophenyl)amino Derivatives

(a) 2-Nitrobenzyl Derivatives

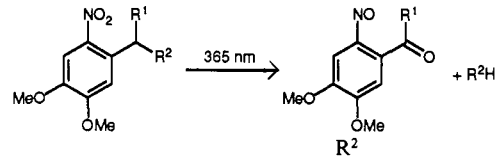

R^1	R^2	Φ[a]
H[b]	OH	0.10
H[b]	$OCOCH_3$	0.005
H[b]	OCH_3	0.09
H[b]	NH_2	0.26[c,d]
H[b]	NH_3^+	<0.002[d,e]
H[b]	$NHCOCH_3$	0.05[f]
2-nitro-4,5-dimethoxyphenyl[g]	OH	0.12
2-nitro-4,5-dimethoxyphenyl[g]	$OCOCH_3$	0.025
2-nitro-4,5-dimethoxyphenyl[g]	OCH_3	0.10

(b) (2-Nitrophenyl)amino Derivatives

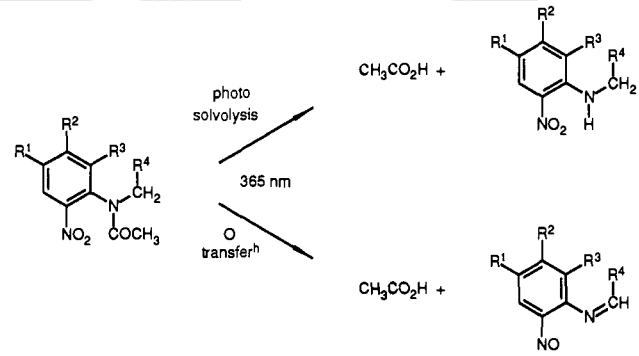

acetamide of	R^1	R^2	R^3	R^4	Φ[i]	mechanism
5,7-dinitroindoline[j]	NO_2	H	$-CH_2-$		0.50	photosolvolysis[14b]
5-bromo-7-nitroindoline[j]	Br	H	$-CH_2-$		<0.01	photosolvolysis[14b]
N-methyl-4,5-dimethoxy-2-nitroaniline[j]	OMe	OMe	H	H	0.045[a]	oxygen transfer[14a]
6,8-dinitro-1,2,3,4-tetrahydroquinoline[j]	NO_2	H	$-CH_2CH_2-$		0.025	oxygen transfer[14a]

[a] Quantum efficiency for loss of starting material (quantified following HPLC separation) after irradiation of 10–20 μM solutions ($A_{365} < 0.1$) at 365 nm in CH_3CH-H_2O (3:7, v/v) at 20 °C. [b] Extinction coefficient $\sim 5 \times 10^3$ M^{-1} cm^{-1} at 365 nm. [c] pH 4 (NH_4HCO_3 buffer). [d] Photoproduct expected to be NH_3. [e] pH 10 buffer (NH_3). [f] Photoproduct expected to be CH_3CONH_2. [g] Extinction coefficient $\sim 8.7 \times 10^3$ M^{-1} cm^{-1} at 365 nm. [h] Proposed mechanism.[12a] [i] Quantum efficiency measured by absorbance changes upon photolysis at 365 nm in CH_3CN-H_2O (3:7, v/v) at 20 °C. [j] Extinction coefficient $\sim 3.5 \times 10^3$ M^{-1} cm^{-1} at 365 nm. See Experimental Section for details.

Table II shows the quantum yields of photorelease of acetic acid from several cyclic and acyclic acetamides. Photolysis of the 5,7-dinitroindoline derivative proceeded with an efficiency at least 1 order of magnitude greater than any of the other groups (ester or amide) evaluated, perhaps because the mechanism involves photosolvolysis rather than intramolecular oxygen transfer.[14b]

The monoester derivatives of BAPTA (Scheme I, Table I) were conveniently prepared by acylating the parent alcohol with BAPTA bis(anhydride). The 2-nitroanilides required a more tedious route through *N*-bromoacetylation of the much less nucleophilic parent amine, monoalkylation of bis(2-aminophenoxy)ethane followed by trialkylation with *tert*-butyl bromoacetate and subsequent selective cleavage (BF_3–HOAc) of the three esters. All BAPTA esters or amides (Scheme I) gave very low quantum yields of photoconversion of BAPTA, often unmeasurable, with the best being the monoester of BAPTA with bis(4,5-dimethoxy-2-nitrophenyl)methanol (**1a**, Table I). Its absorbance spectrum was essentially a summation of the spectra of BAPTA and bis(4,5-dimethoxy-2-nitrophenyl)methanol. The low Ca^{2+} affinity of the ester was conveniently measured by monitoring the effect of Ca^{2+} on the BAPTA contribution to the absorption spectrum at 250 and 290 nm.[11] Photolysis of the bis(4,5-dimethoxy-2-nitrophenyl)methyl group at 365 nm gave absorbance changes consistent with the expected formation of 4,5,4′,5′-tetramethoxy-2-nitro-2′-nitrosobenzophenone and free BAPTA. Titration of the released chelator indeed revealed a Ca^{2+} affinity similar to that of BAPTA[11] (Table I). The reaction proceeded cleanly, as judged by isosbestic points in successive spectra during photolysis, but the quantum yield was very low (0.0071).

Despite the promising photolysis efficiency of *N*-acetyl-5,7-dinitroindoline, the corresponding BAPTA amide **1f** only photolyzed in saturating Ca^{2+} (Scheme I, Table I) and hence would be ineffective in lowering $[Ca^{2+}]$ unless the latter were already extremely high.

Another photosensitive protecting group investigated was (8-azido-4-methoxynaphthyl)-1-methyl, whose acetate ester is reported to release acetic acid following intramolecular nitrene insertion and formation of benz[*c*]indole.[16] This approach proceeded smoothly with the acetate model, but with BAPTA **1e** failed to release the free chelator in zero Ca^{2+}. Instead, the unidentified photoproduct showed no affinity for Ca^{2+}.

We then considered manipulating the affinity of the chelator through electronic rather than steric effects, by introducing an electron-withdrawing diazoketone onto the benzene ring, which photochemically converts to the electron-donating carboxymethyl group by the Wolff rearrangement. Our first compound of this design, "diazo-1" (**2a,b**, Table I) incorporated the diazoketone into one of the benzene rings of BAPTA to form a quinone diazide, which should photorearrange with ring contraction.[17] The compound was synthesized by Teuber oxidation of a BAPTA phenol derivative with potassium nitrosodisulfonate to give the *o*-quinone.[18] Base elimination of the tosylhydrazone[19] afforded the

(16) Barton, D. H. R.; Sammes, P. G.; Weingarten, G. G. *J. Chem. Soc. C* **1971**, 721–728.

(17) (a) Ershov, V. V.; Nikiforov, G. A.: de Jonge, C. R. H. In *Quinone Diazides, Studies in Organic Chemistry*; Elsevier: New York, 1981; Vol. 7. (b) Meier, H.; Zeller, K.-P. *Angew. Chem., Int. Ed. Engl.* **1975**, *14*, 32–43.

Scheme III

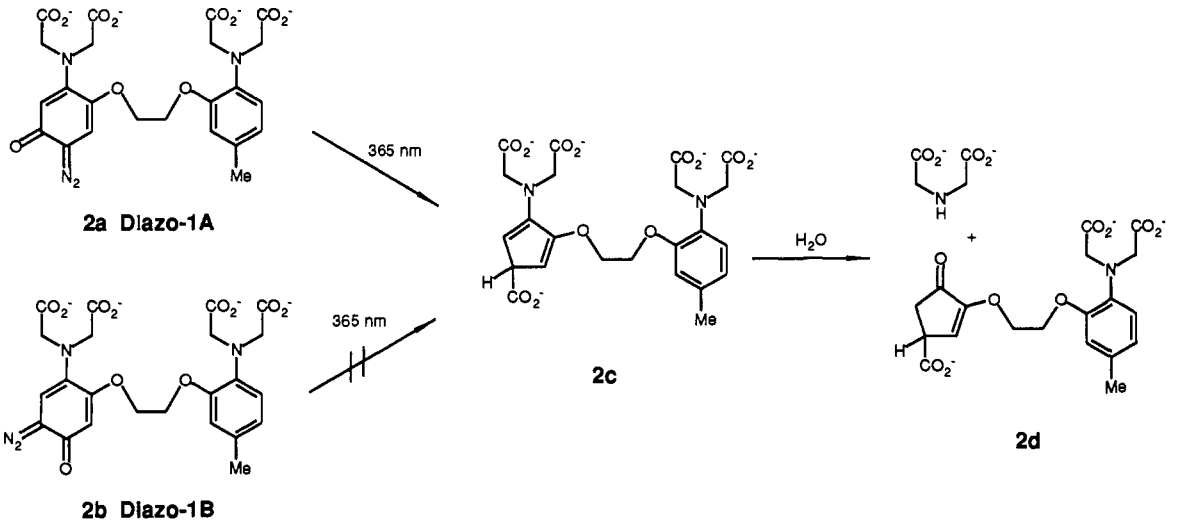

Scheme IV, Synthesis of Diazo-2[a]

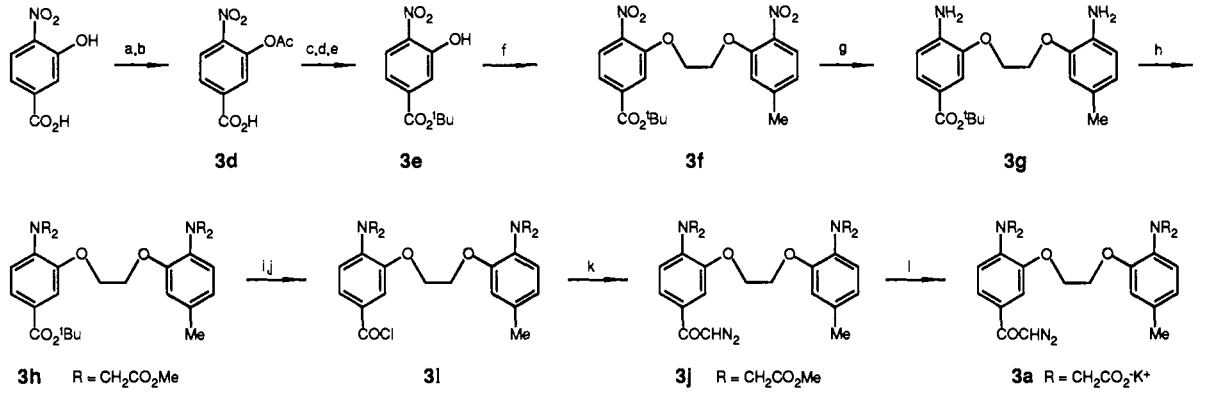

[a] Reagents and conditions: (a) Ac_2O, pyridine; (b) aqueous $NaHCO_3$; (c) $SOCl_2$; (d) *t*-BuOH, pyridine, $CHCl_3$; (e) aqueous $NaHCO_3$ plus MeOH; (f) 1-bromo-2-(5-methyl-2-nitrophenoxy)ethane, K_2CO_3, DMF; (g) H_2, catalytic Pd/C, EtOAc–EtOH, 1 atm, 20 °C; (h) $BrCH_2CO_2Me$, 1,8-bis(dimethylamino)naphthalene (Proton Sponge, Aldrich); (i) CF_3CO_2H, CH_2Cl_2; (j) $(COCl)_2$, CH_2Cl_2; (k) CH_2N_2, Et_2O; (l) aqueous KOH plus MeOH.

diazoketone as a mixture of two isomers. The major product following saponification, diazo-1A, has its absorbance peak at ~350 nm, which shifts to shorter wavelengths on binding Ca^{2+}. This is indicative of strong electronic interaction between the carbonyl group and the chelating amino group, indicating isomer **2a** (Scheme III) and, as expected, resulted in a very low affinity for Ca^{2+} (K_d = 176 μM). Photolysis at 365 nm is very efficient (quantum yield is 0.82 and >0.9 in low and high Ca^{2+}, respectively) and results in a sizable decrease in absorbance at that wavelength, with a small broad absorbance increasing at 500 nm. On binding Ca^{2+}, the postphotolysis absorbance changes at 250 and 280 nm but not at 365 or 500 nm; however, the measured Ca^{2+} affinity is virtually unchanged ($K_d \approx 200$ μM). The other isomer of the quinone diazide, diazo-1B (see Scheme III), following saponification has a small absorbance peak at 350 nm ($\epsilon \approx 5000$ M^{-1} cm^{-1}) and a very broad band at ~500 nm. On binding Ca^{2+}, the absorbance decreases at 250 and 300 nm but is unchanged at 350 and 500 nm. This suggests little electronic interaction between the chelating amino group and the carbonyl group on the diazo group, suggesting structure **2b** for diazo-1B (Scheme III). Ca^{2+} binding is correspondingly strong, with $K_d \approx 150$ nM. The tetraanion is weakly, if at all, photosensitive at 365 nm. Because of the low extinction at that wavelength, photolysis proceeds slowly. Thus diazo-1A (**2a**) is photosensitive but does not increase its Ca^{2+} affinity, whereas diazo-1B (**2b**) starts with too high a Ca^{2+} affinity and is hardly photolabile.

Chart I

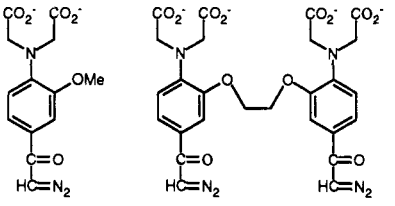

Ultimately the successful approach was to place the diazoketone as a substituent to the aromatic ring in conjugation with the amine (Scheme II) to yield diazo-2. Initial synthetic routes to diazo-2 focused on oxidation of the readily available *p*-formyl BAPTA to *p*-carboxy BAPTA, the key intermediate (Scheme IV, structure **3h**), but all efficacious methods[20] also oxidized the sensitive amine group. Friedel–Crafts carboxylation[21] of BAPTA tetraester with phosgene or oxalyl chloride also failed. Eventually, the *p*-carboxy BAPTA was constructed stepwise from 3-hydroxy-4-nitrobenzoic acid. An Arndt–Eistert reaction of the acid chloride (**3i**) with diazomethane yielded the ester of the desired product, diazo-2 (**3j**, Scheme IV). Mild base saponification yielded the chelator

(18) Reviewed by: Zimmer, H.; Lankin, D. C.; Horgan, S. W. *Chem. Rev.* **1971**, *71*, 229–246.
(19) Horner, L.; Dürckheimer, W. *Chem. Ber.* **1962**, *95*, 1206–1218.
(20) Lee, D. G. In *Oxidation*; Augustine, R. L., Ed.; Dekker: New York, 1969; pp 81–86.
(21) Olah, G. A.; Olah, J. A. In *Friedel–Crafts and Related Reactions*; Olah, G. A., Ed.; Interscience: New York, 1964; Vol. 3, pp 1257–1273.

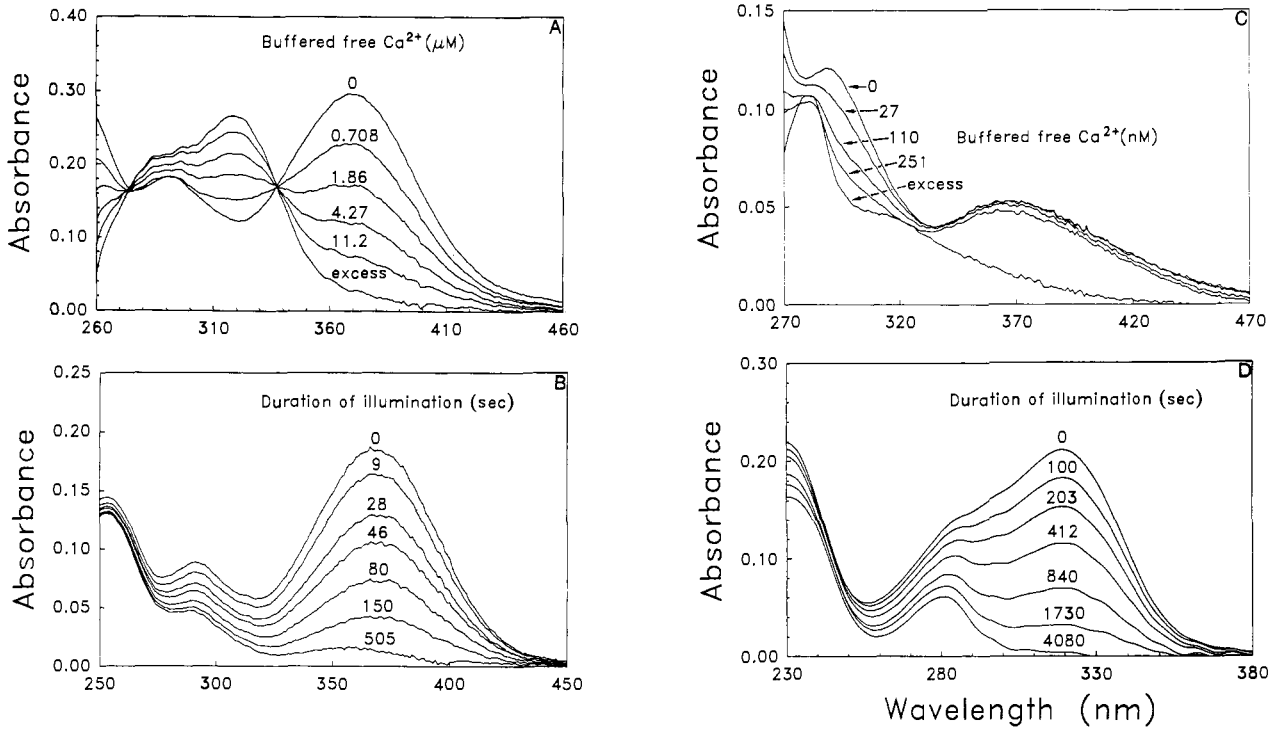

Figure 1. (A) Absorbance spectra of unphotolyzed diazo-2 as a function of free $[Ca^{2+}]$. The titration was done at 22 °C with 10 mL of 100 mM KCl, 10 mM K·MOPS, 10 mM K_2H·HEEDTA, and 14 μM diazo-2 as starting materials, adjusting the pH to 7.24, recording the spectrum, and then discarding 1.0 mL of this solution and replacing with 1.0 mL of 100 mM KCl, 10 mM K·MOPS, 10 mM KCa·HEEDTA, 14 μM diazo-2, readjusting the pH to 7.24, and recording the spectra, which was then in 9 mM K_2H·HEEDTA. Subsequent iterations to reach n mM KCa·HEEDTA, $(10 - n)$ mM HEEDTA, n = 2–10, were done by discarding $10.0/(11 - n)$ mL and replacing with equal volumes of the 10 mM KCa·HEEDTA, 14 μM diazo-2 stock. After n = 10 had been reached to give a free Ca^{2+} between 10^{-5} and 10^{-4} M, addition of 1 mM $CaCl_2$ had no further effect on the spectrum. For clarity, only six spectra are included in the figure, n = 0, 2, 4, 6, 8, and 10. Each spectrum is labeled with the calculated free $[Ca^{2+}]$ imposed by the HEEDTA buffer, assuming a log effective stability constant[39] of 5.55 at pH 7.24. (B) Absorbance spectra of diazo-2 undergoing photolysis in the absence of Ca^{2+}. Diazo-2 was dissolved at 8 μM in 100 mM KCl, 10 mM Tris, 5 mM MOPS, 4 mM K_2H_2EGTA and pH titrated to 7.2 with HCl. Spectra were obtained after 0, 2, 5, 9, 16, 28, 46, 80, 150, 285, 505, and 903 s of 365-nm illumination at 7.82×10^{-9} einstein cm^{-2} s^{-1} from the Spectroline lamp. For clarity only the 0-, 9-, 28-, 46-, 80-, 150-, and 505-s spectra have been reproduced here. The 505- and 903-s spectra were identical, confirming completion of photolysis after those times. Solutions were at 22 ± 2 °C. (C) Absorbance spectra of phenylacetate (photolyzed diazo-2) as a function of free $[Ca^{2+}]$. The phenylacetate was produced by irradiating a 30 μM solution of diazo-2 in 100 mM KCl, 10 mM Tris-HCl, 10 mM K_2H·HEEDTA, pH 8.40, with the Spectroline lamp at 365 nm to completion. The titration was then performed as in A but the pH was maintained at 8.40, at which the calculated log effective stability constant[39] for HEEDTA was 6.60. (D) Absorbance spectra during photolysis of the Ca^{2+} complex of diazo-2. The method was as described in B except that the EGTA was replaced by 2 mM $CaCl_2$, and spectra were measured after 0-, 50-, 100-, 203-, 412-, 840-, 1730-, 4080-, and 8000-s illumination. The last two spectra were identical, confirming completion. For clarity, the 50- and 8000-s spectra have been omitted.

tetraanion. Although this was unstable in strong aqueous base or acid (pH >13 or pH <4), it was possible to prepare concentrated aqueous solutions of the anion for microinjection into cells, as well as the tetrakis(acetoxymethyl)ester for nondisruptive loading via intracellular esterases.

Diazo-3 and diazo-4 (structures **4a** and **5a**, Chart I) were synthesized by an analogous route.

Absorbance, Ca^{2+}-Binding, Photolysis, and Quantum Yield. Because of the direct conjugation of the dialkylamine moiety with the diazoketone group, diazo-2 has a large absorbance in the 350–400-nm range, which shifts 50 nm to shorter wavelengths on binding Ca^{2+} (Figure 1A). The dissociation constant for Ca^{2+} is relatively high, at 2.2 μM, due to the electron-withdrawing ability of the carbonyl group. In zero Ca^{2+}, photolysis occurs at 365 nm with a quantum yield of 0.030. The peak at 370 nm decreases to near base line, giving a spectrum similar to that of unsubstituted BAPTA, although a small peak remains at 355 nm (Figure 1B). Binding of Ca^{2+} now produces absorbance changes similar to those observed with BAPTA (Figure 1C); interestingly, the peak at 355 nm is only affected by $>10^{-6}$ M Ca^{2+}. A Hill plot indicates an affinity of 73 nM after photolysis, as expected for **3c** (Scheme II), in which the carboxymethyl substituent is weakly electron-donating. Some deviation of the plots from linearity suggests a side product with a dissociation constant of $\sim 10^{-6}$ M. The expected side product of the Wolff rearrangement is the *p*-(2-hydroxyacetyl) derivative formed through insertion of the intermediate carbene into the O–H bond of H_2O. Reaction of diazo-2 with dilute aqueous acid should give the same product whose absorbance spectrum indeed matched that of the residual peak at 355 nm after photolysis in low Ca^{2+}. Dilute acid probably converts the diazoketone quantitatively to the hydroxyacetyl derivative, since the process shows sharp isosbestic points and the resulting product displays a complete lack of photosensitivity. Once the extinction coefficient for the hydroxyacetyl derivative was known, the amount of the side product arising from photolysis could be calculated to be ~10%. Photolysis in saturating Ca^{2+} (Figure 1D) occurs with a somewhat higher quantum yield (0.057).

Diazo-3 was synthesized as a control for any deleterious effects of the intermediate ketocarbene (**3b**, Scheme II) or acid release from the phenylacetic acid product (**3c**, Scheme II) in biological experiments with diazo-2. Diazo-3 contains the photosensitive moiety of diazo-2 but, lacking half of the cation coordinating site (structure **4a**, Chart I), has negligible affinity for Ca^{2+} ($K_d > 10^{-3}$ M, Table I). Diazo-4 has a diazoacetyl group incorporated into each of the benzene rings of BAPTA and gives a much larger change in affinity for Ca^{2+} upon photolysis (1600-fold) at the expense of lowered quantum yield (structure **5a**, Chart I, Table I), which is approximately half that of diazo-2, as two diazoketones groups must be photolyzed for complete conversion.

Flash Photolysis Kinetics in Vitro. When a diazoketone is photolyzed in aqueous solution the major ultimate product is a carboxylic acid. In the present case, a substituted phenylacetic acid with an expected pK_a close to 4.5 is generated (structure **3c**,

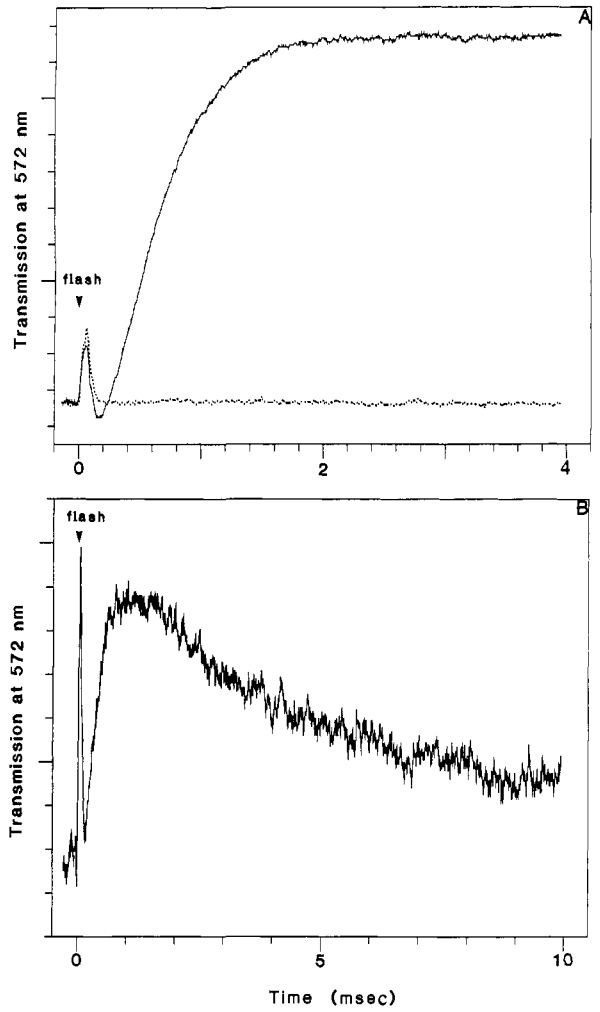

Figure 2. (A) Kinetics of generating high-affinity chelator as signaled by acid release following flash photolysis of diazo-2. Diazo-2 was dissolved at 70 μM concentration in 100 mM KCl, 40 μM BAPTA, and enough cresol red to yield OD_{572} = 0.1 after the solution has been adjusted to pH 8. Transmitted light intensity at 572 nm was monitored by use of an Hg–Xe arc lamp, a monochromator, a photomultiplier, and a Biomation transient recorder. Each small division of the ordinate corresponds to 0.002 absorbance unit. The small upward spike at time zero is an optical artifact from the xenon flash lamp. The solid trace is from the sample containing diazo-2. For comparison, the dotted trace is from a photochemically inert sample containing cresol red in 100 mM KCl at pH ~8. This control record shows that the flash artifact is clearly separable from the gradual decrease in absorbance of the cresol red as acid is released during the dark reaction following flash photolysis of diazo-2. (B) Kinetics of Ca^{2+} uptake by photolyzed diazo-2. The sample contained 70 μM diazo-2, 2 mM HEEDTA, 1 mM $CaCl_2$, 100 mM KCl, and cresol red to give OD_{572} = 0.1 after the solution was adjusted to pH 8 under helium purge. Monitoring of the light transmission at 572 nm was performed as for A. Each small division of the ordinate corresponds to 3.4 × 10^{-4} absorbance unit. The spike at time zero is an optical artifact generated by the xenon flash lamp. As the acid form of the high-affinity chelator was generated following flash photolysis, the solution transiently acidified, as revealed by the decrease in cresol red absorbance (rise in transmitted light intensity). As the photolyzed diazo-2 took Ca^{2+} away from HEEDTA, the freed HEEDTA bound protons and thus alkalinized the solution, a process reflected by the increase in cresol red absorbance (decline in light transmission at 572 nm).

Scheme I). Product formation is thus accompanied by proton release, which is readily monitored spectroscopically if a suitable acid–base indicator is used. In our experiments, we chose to use cresol red (pK_a 8.2) to monitor proton release following flash photolysis of the diazo compounds in aqueous solutions adjusted to pH 8. Figure 2A shows a typical diazo-2 flash photolysis trace where the transmittance of cresol red in the sample was monitored at 572 nm. The absorbance of cresol red at 572 nm decreases with decreasing pH. As the carboxylic acid product, **3c**, is generated, the solution acidifies and the *transmittance* of the sample is expected to rise. As revealed by the exponentially rising trace in Figure 2A, a transmittance increase due to acidification was indeed the dominant effect observed following flash photolysis of diazo-2 in aqueous solution. The chemical structure of the photolabile chromophore in diazo-3 is essentially identical with that in diazo-2 (Chart I). Correspondingly, flash photolysis of diazo-3 under identical conditions yielded experimental traces that were qualitatively the same as those obtained for diazo-2. In Table I, we present the characteristic time constants for carboxylic acid formation following flash photolysis of diazo-2 and diazo-3. Flash photolysis of Ca^{2+}-bound diazo-2 produced the carboxylic acid with a characteristic time of 134 μs. The time slowed to 433 μs when Ca^{2+}-free diazo-2 was photolyzed. Diazo-3, with negligible pre- and postphotolysis affinity for Ca^{2+} (K_d's >10^{-3} M), yielded product with a time constant of 239 μs, intermediate between those found for the Ca^{2+}-bound and Ca^{2+}-free forms of diazo-2.

As shown in Figure 2A, the flash photolysis record reveals a small alkalinization prior to carboxylic acid generation. This transient decrease in transmittance at 572 nm was observed for both diazo-2 and diazo-3. The transmittance dip is not a result of photochromism of the acid–base indicator or the photoproducts, since flashing a control sample containing cresol red and either no diazo compound or exhaustively photolyzed material produced no corresponding effect. The dip is also not the result of a strongly absorbing, long-wavelength photochemical intermediate en route to the carboxylic acid product or the hydroxyketone side product, as flash photolysis of a solution of diazoketone in the absence of cresol red did not show the effect. Finally, the transient alkalinization is likely due to a first-order or pseudo-first-order process since changing the concentration of diazo-3 by a factor of 2 produced no significant change in the time constant of the process, being 48 ± 3 μs at 35 μM diazo-3 and 59 ± 8 μs at 70 μM diazo-3. It should be noted that since the pulse width of our flash was 85 μs, the signal due to the fast alkalinization overlapped with the decay of the flash artifact. Consequently, it was quite difficult to assess accurately either the decay time or the amplitude of the alkalinization signal. The time constants given above for the alkalinization process should thus be regarded as approximate values.

Having determined the rate at which the high-affinity chelator was photochemically generated from diazo-2, we proceeded to examine the kinetics of Ca^{2+} binding and release by photolyzed diazo-2, relying on the 1:1 competition between protons and Ca^{2+} for the chelator HEEDTA:

$$H{\cdot}HEEDTA^{-2} + Ca^{2+} = Ca{\cdot}HEEDTA^{-} + H^{+}$$

If diazo-2 is photolyzed in the presence of HEEDTA partially saturated with Ca^{2+}, the photogenerated **3c** would take some Ca^{2+} away from HEEDTA. The newly freed HEEDTA would then take up some protons and lead to an alkalinization of the sample. The shift in Ca^{2+}-binding equilibrium could thus be visualized with an indicator like cresol red. Control experiments (not shown) indicated that at HEEDTA buffer concentrations of ≥2 mM, the intrinsic kinetics of the Ca^{2+}–HEEDTA equilibrium was no longer limiting the speed of the final alkalinization.

Figure 2B shows the flash photolysis of 70 μM diazo-2 plus 2 mM HEEDTA half-saturated with Ca^{2+} to give a calculated free [Ca^{2+}] of 377 nM. It can be seen that the solution first acidified owing to the formation and dissociation of the product carboxylic acid but subsequently began realkalinizing as the newly formed product chelator competed with HEEDTA for Ca^{2+}. The time constant of the realkalinization was 2.8 ms (Table I). Since [Ca^{2+}] was almost perfectly clamped by the HEEDTA, this time constant should equal $(k_{on}[Ca^{2+}] + k_{off})^{-1}$, where k_{on} is the bimolecular rate constant for the binding of Ca^{2+} by **3c**, k_{off} is the unimolecular rate constant for dissociation of the complex between **3c** and Ca^{2+}, and [Ca^{2+}] is the 377 nM free Ca^{2+} concentration as set by the dominant HEEDTA buffer.[22] From equilibrium

(22) Bernasconi, C. F. *Relaxation Kinetics*; Academic: New York, 1976; pp 12–13.

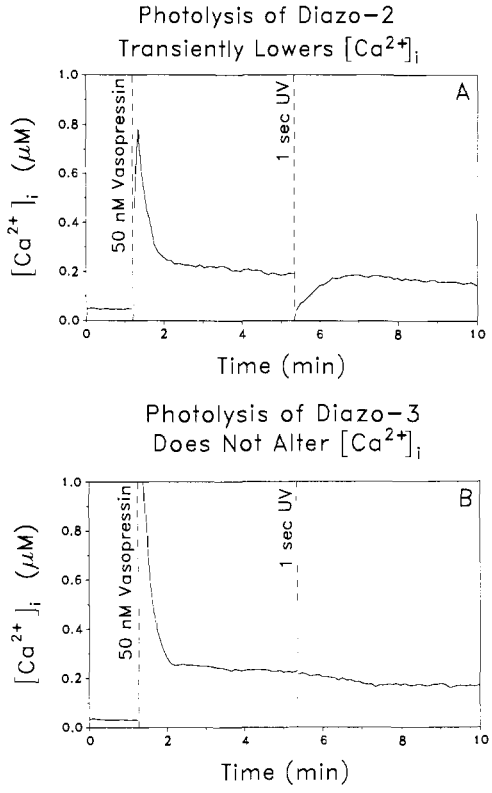

Figure 3. (A) Rapid Ca^{2+} sequestration by flash-photolyzed diazo-2 in a Fisher rat embryo fibroblast cell. Prior to the start of data acquisition, the REF52 fibroblast cell was loaded with fluo-3 and diazo-2 by incubation for 30 min at 25 °C in DME medium containing 1 μM diazo-2 AM and 10 μM fluo-3/AM. Acquisition of fluo-3 fluorescence intensity images was begun at time 0. The fluorescence intensity data were converted to intracellular Ca^{2+} concentrations by a calibration procedure previously described.[9b] The event markers correspond to (1) stimulating the cell with 50 nM [Arg^8]vasopressin and (2) flashing the cell for 1 s with UV light. (B) A control experiment to show that the $[Ca^{2+}]$ drop in (A) required the entire Ca^{2+}-binding site of diazo-2 and was not an artifact arising from the chemistry of diazoacetyl group photolysis. The experimental conditions were the same as in (A) except that the cell was loaded with fluo-3 and diazo-3 (instead of diazo-2) by incubation for 90 min at 25 °C in DME medium containing 10 μM fluo-3/AM and 1 μM diazo-3/AM. The event markers correspond to (1) stimulating the cell with 50 nM [Arg^8]vasopressin and (2) flashing the cell for 1 s with UV light.

measurements on **3c**, we know K_d ($=k_{off}/k_{on}$) = 73 nM (Table I). Therefore, for photolyzed diazo-2, $k_{on} = 8.0 \times 10^8$ M^{-1} s^{-1} and $k_{off} = 58$ s^{-1}.

Biological Testing of Diazo-2. Biological testing of the ability of diazo-2 to take up Ca^{2+} is shown in Figure 3A. Prior to the start of data acquisition ($t = 0$), the REF52 fibroblast cell was loaded with diazo-2 and fluo-3. Fluo-3 is an indicator whose fluorescence is excited by visible wavelength light that does not affect the diazo compounds. Its fluorescence quantum yield is enhanced about 40-fold by Ca^{2+} binding, which occurs with a K_d of 400 nM.[9a] At the time marked in Figure 3A by the first dashed line, the cell was stimulated with 50 nM [Arg^8]vasopressin, which elicted a sharp but transient rise in $[Ca^{2+}]_i$, which declined to a plateau value (~200 nM) that was higher than the prestimulation resting $[Ca^{2+}]_i$. At the time marked by the second dashed line, the cell was illuminated with 1 s of UV, which control experiments showed was sufficient to photolyze all of the diazo-2 in the cell. The Ca^{2+}-binding efficacy of photolyzed diazo-2 is evident as $[Ca^{2+}]_i$ dropped precipitously to ~50 nM immediately after photolysis. The cell subsequently restored $[Ca^{2+}]_i$ back up to the poststimulation plateau level.

Since diazo-2 photolysis proceeds through reactive photochemical intermediates and, at physiological pH, generates a proton for each molecule of high-affinity chelator produced, it is important to control for all the chemical effects of diazo-2 photolysis that have nothing to do with Ca^{2+} sequestration. Diazo-3 is ideally suited for this purpose because, except for its inability to bind Ca^{2+}, its chemistry is identical with that of diazo-2. Figure 3B shows results from an experiment analogous to that presented in Figure 3A except that the cell had been loaded with diazo-3 instead of diazo-2. It can be seen from Figure 3B that the response of the cell to [Arg^8]vasopressin is similar to that seen in Figure 3A; however, UV photolysis of intracellular diazo-3 did not have any effect on the intracellular Ca^{2+} concentration.

Covalent Modification of Lysine by Photochemical Intermediates. HPLC analysis revealed that when 100 μM diazo-3 was photolyzed in the presence of 100 mM lysine hydrochloride at pH 7.2, aside from the main peak attributable to photolyzed diazo-3, ~6% of the total absorbance could be found under a new peak, which was absent when diazo-3 was photolyzed in KCl. We have attributed the new peak to lysine that has been covalently modified by a reactive intermediate generated by photolysis of diazo-3. If we assume that the normal photoproduct and the lysine-modified photoproduct have comparable extinction coefficients, then we can calculate that ~6 μM of the modified lysine was produced, i.e., lysines were covalently modified at a frequency of $\sim 6 \times 10^{-5}$.

Discussion

Photochemical Strategy and Chelator Properties. The disappointingly low quantum yields of photolysis for the nitrobenzyl models (Table II) are in agreement with recently reported values for methoxy-substituted 2-nitrobenzyl carbamates.[23] 2-Nitrobenzyl esters, however, are much more photolabile, with quantum yields of 0.08–0.20,[15b] but unfortunately the 2-nitrobenzyl (data not shown) and 4,5-dimethoxy-2-nitrobenzyl esters of BAPTA photolyzed very slowly at 365 nm. The presence of another *o*-nitro group might be expected to increase the efficiency of photolysis. This was the case for the bis(4,5-dimethoxy-2-nitrophenyl)methyl ester, although substitution of a phenyl group alone at the benzylic position reportedly gives a 2.5-fold increase in quantum efficiency.[15b] Placing the nitro groups on the same phenyl ring increased quantum yield but reduced the extinction as well.[4b,23a] BAPTA bis(4,5-dimethoxy-2-nitrophenyl)methyl ester (**1a**), while the most successful of the nitrobenzyl esters, would still require too much irradiation for biological use. Tertiary amines are known to be able to quench nitro excited states, possibly through a charge-transfer intermediate.[24] The presence of two separate nitro groups in the bis(4,5-dimethoxy-2-nitrophenyl) group may partially explain why it is the least quenched by the BAPTA moiety.

A somewhat different proximity effect of BAPTA was seen with the naphthalene azide protecting group **1e**, where photolysis occurred with high efficiency, but the reactive nitrene intermediate inserted presumably in the BAPTA moiety rather than the *peri*-methylene group as needed to release BAPTA.

A second approach to the problem of producing a Ca^{2+} chelator that increases its affinity on irradiation was more successful. In analogy with the "nitr" series of chelators, the affinity of the chelator was manipulated by remote electronic effects rather than by steric control of the coordination site.[4a,b] The general idea was to incorporate an electron-withdrawing diazoketone, which is photolyzed to an electron-donating carboxymethyl group via a Wolff rearrangement. Table I shows the resulting diazo chelators and the order in which they were prepared. Diazo-1A (structure **2a**, Scheme III) is a quinone diazide, whose Ca^{2+} affinity was expected and found to be very low. Photochemical rearrangement was expected to result in a 1-carboxycyclopentadiene derivative (structure **2c**, Scheme III), but no high-affinity Ca^{2+} chelator was in fact produced on photolysis. We suggest that the enamine photoproduct was rapidly hydrolyzed to the cyclopentenone derivative **2d** and iminodiacetic acid (Scheme III), resulting in Ca^{2+} dissociation constants of ~10^{-4} M. Diazo-1B (structure **2b**, Scheme III), in which only the diazo group is in conjugation with the chelating amino group, has too high a starting Ca^{2+} affinity

(23) (a) Cummings, R. T.; Krafft, G. A. *Tetrahedron Lett.* **1988**, *29*, 65–68. (b) Krafft, G. A.; Sutton, W. R.; Cummings, R. T. *J. Am. Chem. Soc.* **1988**, *110*, 301–303.

(24) Döpp, D. *Top. Curr. Chem.* **1975**, *55*, 49–85.

for biological application and was only weakly photosensitive.

To prevent enamine formation, the diazoketone group was shifted outside of the aromatic ring to give diazo-2, thus ensuring retention of the phenyl group's aromaticity throughout the photoreaction and subsequent dark reaction. Diazo-2 worked reasonably successfully; the electron withdrawal of the diazoacetyl group weakened the Ca^{2+} affinity of BAPTA to a K_d of 2.2 μM. Photolysis produced a 30-fold increase in affinity, to a K_d of 73 nM. The affinity of Mg^{2+} is weak and changes only 1.6-fold upon photolysis, so that perturbations of intracellular free $[Mg^{2+}]$ are likely to be negligible. The quantum yield for photolysis is modest, but the high extinction at 370 nm results in satisfactory rates of photolysis, several times faster than nitr-5, which has been photolyzed successfully in cells without noticeable irradiation damage. The quantum yield is consistent with literature values for diazoacetophenone when the longest wavelength absorption band (assigned to a forbidden transition) is excited.[17b,25] Reversing the position of the diazo and carbonyl group to produce a (methoxycarbonyl)diazomethyl substituent [i.e., $CH_3OCOC(N_2)$] in model compounds greatly increased the quantum yield but resulted in a considerably lower extinction coefficient in the long-wavelength UV, making it inferior overall. The difference in quantum yield of the Ca^{2+}-bound and Ca^{2+}-free forms of diazo-2 is probably due to the deactivating effect of the *p*-amino group on the photochemistry, which is greatly reduced when Ca^{2+} is bound to the iminodiacetate group to make the nitrogen tetrahedral.[4a,b] This Ca^{2+}-dependent behavior is analogous to that observed in the nitr chelators,[4a,b] the 5,7-dinitroindolinyl amide of BAPTA (**1f**), and to the Ca^{2+}-dependent fluorescence quantum yields of related indicator dyes.[11,26]

Diazo-4, which has a diazoacetyl substituent on each of the aromatic rings of BAPTA (structure **5a**, Chart I) and shows a much greater change in Ca^{2+} affinity (1600-fold) upon complete photolysis (Table I), was made for certain biological applications that require decreasing $[Ca^{2+}]_i$ from $\geq 10^{-5}$ to $\sim 10^{-7}$ M. Diazo-2 in such circumstances either would prevent high $[Ca^{2+}]$ levels even before photolysis or would become Ca^{2+}-saturated and be unable to generate free high-affinity chelator to lower $[Ca^{2+}]_i$. However, the intermediate in the photolysis of diazo-4 (in which only one diazoacetyl group is photolyzed) will have a similar affinity to unphotolyzed diazo-2, so to jump from $\sim 10^{-5}$ to $\sim 10^{-7}$ M in free $[Ca^{2+}]$ will require almost complete photolysis of all the diazo-4, whereas diazo-2 can be photolyzed partially several times in an experiment.

Diazo-2 and analogues suffer from a similar side reaction to diazo-1, that is, insertion of the ketocarbene intermediate into H_2O, resulting in formation of a hydroxyacetyl-sustituted BAPTA, which is expected to have an affinity slightly higher than diazo-2 and thus will not contribute to the high-affinity Ca^{2+} buffer. However, the extent of this side reaction is only 10% and easily overcome by increasing the concentration of diazo-2 in the experiment. Diazo-4 would be expected to produce 19% low-affinity side product on complete photolysis and approximately 20% was in fact measured by the residual absorbance at 355 nm.

Flash Photolysis Kinetics. The kinetics of acid formation from aryl ketenes in aqueous solution have previously been investigated by Bothe et al.[27] These authors flash-photolyzed various para-substituted diazoacetophenones in aqueous solution and conductometrically monitored the generation of the product phenylacetic acids. They found characteristic time constants ranging from 20 μs for *p*-NO_2 substitution to 265 μs for *p*-CH_3 substitution. In all cases, the postphotolysis increase in solution conductance was found to be single-exponential in character. In contrast, we found in our studies that, following flash photolysis of diazo-2 and diazo-3, two processes could be detected that changed the solution pH: a fast alkalinization followed by a slower acidification corresponding to carboxylic acid generation. The time constants characterizing acid production from diazo-2 and diazo-3 were of the order of one to several hundred microseconds—comparable to the values observed for diazoacetophenones having electron-donating substituents in the para position.[27] The fast transient alkalinization we observed reflected a unimolecular process and appeared to be a direct result of photolyzing diazo-2 or diazo-3. We conclude that the transient alkalinization is a peculiarity arising from the presence of *p*-amino substituent in our molecules, while the kinetics of the subsequent reaction of the ketene with water to generate carboxylic acid agree quite well with the results of Bothe et al.[27]

In studying the photolysis of diazo-2 we found that the time constant for carboxylic acid generation showed a dependence on Ca^{2+} binding—not surprising since diazo-2 is a Ca^{2+} chelator. When not complexed with Ca^{2+}, the amino nitrogen is free to donate its long pair by resonance, but when Ca^{2+} binds to the chelator, the nitrogen, being one of the ligand atoms coordinated to Ca^{2+}, becomes less strongly electron-donating. Since hydrolysis of phenyl ketenes is known to be accelerated by electron-withdrawing substituents and retarded by electron-donating substituents,[27] Ca^{2+}-bound diazo-2 should yield the product carboxylic acid more quickly than the Ca^{2+}-free form after photolysis. These predictions are borne out by the results: acid generation for Ca^{2+}-bound diazo-2 proceeded with a characteristic time of 134 μs, more than 3 times faster than the 433 μs characterizing the same process for Ca^{2+}-free diazo-2.

Since the photolabile moieties in diazo-2 and diazo-3 are essentially identical, the kinetics of acid production following flash photolysis of diazo-3 and Ca^{2+}-free diazo-2 are expected to be comparable, and yet acid production for diazo-2 was 1.8 times slower than for diazo-3. This slower rate for diazo-2 compared to diazo-3 may partly be explained by the presence of four carboxylates in diazo-2 compared to two in diazo-3. The extra negative charges may retard nucleophilic attack by water or OH^- on the ketene. It is also conceivable that the aqueous conformation of diazo-2 may be such that the [(dialkylamino)phenoxy]ethoxy substituent may provide some slight steric hindrance to hydrolysis of the ketene.

Kinetics of Ca^{2+} Binding by Photolyzed Diazo-2. We have also determined the rate constants characterizing Ca^{2+} binding by photolyzed diazo-2 (structure **3c**, Scheme II). At 8.0×10^8 M^{-1} s^{-1}, the biomolecular rate association rate constant for diazo-2 and Ca^{2+} is higher than the corresonding rate constants for structurally similar chelators fura-2 (6.02×10^8 M^{-1} s^{-1}) and azo-1 (3.99×10^8 M^{-1} s^{-1}).[28] However, the unimolecular rate constant for dissociation of the Ca^{2+} complex of photolyzed diazo-2, 58 s^{-1}, is lower than the corresponding values for fura-2 (96.7 s^{-1}) and azo-1 (1177 s^{-1}).[28,29] The opposing trends found for the association and dissociation constants for these three chelators combine to yield the observed trend in the equilibrium dissociation constants for the Ca^{2+} complexes of the three chelators:[26,30]

$$K_d(\text{photolyzed diazo-2}) = 73 \text{ nM} < K_d(\text{fura-2}) = 135 \text{ nM} < K_d(\text{azo-1}) = 2.63 \ \mu\text{M}$$

Biological Application of the Diazo Chelators. The tetrakis-(acetoxymethyl) esters of diazo-2 and diazo-4 as well as the bis(acetoxymethyl) ester of diazo-3 have been synthesized. The acetoxymethyl (AM) groups mask the negative charges on the carboxylate functions, so the AM ester of diazo-2, -3, or -4 can easily diffuse across the cell membrane, which is largely impermeable to ions. Once inside, nonspecific esterases in the cell hydrolytically cleave the AM esters and restore diazo-2, -3, and -4 to carboxylate form, which being polyanions, are trapped within the cell. By this method, cells have been shown to accumulate millimolar levels of other polycarboxylate chelators in the presence of micromolar extracellular levels of the corresponding AM ester.[31] The results depicted in Figure 3A demonstrate that diazo-2 loaded

(25) Kirmse, W.; Horner, L. *Justus Liebigs Ann. Chem.* **1959**, *625*, 34–43.
(26) Grynkiewicz, G.; Poenie, M.; Tsien, R. Y. *J. Biol. Chem.* **1985**, *260*, 3440–3450.
(27) Bothe, E.; Meier, H.; Schulte-Frohlinde, D.; Sonntag, C. *Angew. Chem., Int. Ed. Engl.* **1976**, *15*, 380–381.
(28) Kao, J. P. Y.; Tsien, R. Y. *Biophys. J.* **1988**, *53*, 635–639.
(29) Jackson, A. P.; Timmerman, M. P.; Bagshaw, C. R.; Ashley, C. C. *FEBS Lett.* **1987**, *216*, 35–39.
(30) Tsien, R. Y. *Annu. Rev. Biophys. Bioeng.* **1983**, *12*, 91–116.
(31) Tsien, R. Y.; Pozzan, T.; Rink, T. J. *J. Cell. Biol.* **1982**, *94*, 325–334.

into living cells via the AM ester can sequester Ca^{2+} when photolyzed. Diazo-2 microinjected into cells is also effective in sequestering Ca^{2+} after photolysis (data not shown). However, the use of AM esters eliminates the need for microinjecting living cells. Such microinjection requires considerable technical skill, always causes some injection damage, requires seconds to minutes for each individual cell, and is impossible on small, free-floating cell types.

The possible kinetic limitations of using diazo-2 and diazo-4 in biological systems should be considered. Since the high-affinity Ca^{2+} chelator is generated by hydrolysis of the photoproduct ketene, the rate of Ca^{2+} sequestration will be limited by the rate at which the chelator is produced. Photochemical steps leading to the formation of product ketene from diazoketones are typically fast, being complete in hundreds of nanoseconds.[32] The real limit is the rate at which the ketene is transformed into the carboxylic acid by hydrolysis, a process that, for diazo-2 at 20 °C, has a time constant of 433 μs. Ultimately then, flash photolysis of diazo-2 or diazo-4 should be able to quench Ca^{2+} rises that have rise times on the order of a millisecond or longer. Fortunately, this is fast enough for most biological applications.

Two potential complications should be considered in using diazo-2 or diazo-4 in living cells, and these have to do with aspects of the photochemistry of diazo-2 and diazo-4. The photolyses proceed through very reactive intermediates, ketocarbenes (which may interconvert with oxirenes), which rearrange in hundreds of nanoseconds[32] to ketenes. Since all the intermediates are highly reactive, they might covalently modify biological important substrates and perturb the normal functions of the cell. The second complication arises from the fact that at physiological pH, photolysis of diazo-2 or diazo-4 releases one or two protons, respectively, in addition to generating Ca^{2+}-buffering capacity. Although the intracellular pH is tightly regulated by the cell (tens of millimolar levels of pH buffering exist in normal cells), small pH excursions can have relatively profound effects.

The first problem, that of reactive intermediates, is probably not serious, since even in the intracellular environment, water is still by several orders of magnitude the most abundant reagent. Indeed, in experiments where 100 μM diazo-3 was photolyzed in the presence of 100 mM lysine hydrochloride at pH 7.2, we found very low levels of covalent lysine modification—6 lysines in 10^5 were covalently modified. Acidification by the photoproduct of diazo-2 or diazo-4 is perhaps a more serious problem, since innumerable biochemical processes are dependent on pH. For both concerns, diazo-3 is an important control compound. Diazo-3 manifests all of the same chemical aspects as diazo-2 *except* Ca^{2+} binding. Diazo-3 is thus the ideal compound to control for all of the chemical effects of diazo-2 or diazo-4 that are unrelated to Ca^{2+} chelation. Indeed, the results shown in Figure 3B demonstrate that photolysis of intracellularly trapped diazo-3 had no detectable effect on Ca^{2+} homeostasis in the REF52 fibroblast cell. Finally, we should state that diazo-3 is a perfectly good "caged proton" in its own right and can be used photochemically to study the effects of transient pH drops on cellular physiology. An advantage of diazo-3 over other "caged protons"[5] is its ready loading and accumulation in cells by incubation with the cell-permeant AM ester.

Experimental Section

Chemicals and solvents (HPLC grade) were used directly as obtained unless otherwise noted. $CHCl_3$ was redistilled from P_2O_5, dimethylformamide and *N*-methyl 2-pyrrolidinone were dried over 4A molecular sieves, and thionyl chloride, *tert*-butyl alcohol and pyridine were redistilled.

Proton magnetic resonance spectra were recorded on a Varian EM-390 90-MHz spectrometer in $CDCl_3$ unless otherwise noted, and the chemical shifts are given in δ values for Me_4Si. UV absorbance spectra were recorded on a Cary 210 or a Perkin-Elmer Lambda Array 3840 spectrophotometer at 20 ± 2 °C. Melting points are uncorrected. Elemental analyses were performed by the Microanalytical Laboratory in the Department of Chemistry at Berkeley.

Thin-layer chromatography (TLC) was carried out on precoated silica gel 60F-254 (E. Merck) or reverse-phase (RP-18, F-254, E. Merck, or $MKC_{18}F$, Whatman) plates. For column chromatography, silica gel 60 (230–400 mesh, E. Merck) was used. All manipulations of compounds sensitive to near-ultraviolet light were performed under an orange safety lamp.

BAPTA Anhydride. BAPTA free acid (Lancaster Synthesis) (476 mg, 1 mmol) was suspended in acetic anhydride (3 mL) and pyridine (162 μL, 2 mmol) and heated at 60–70 °C for 1 h. The resulting pale brown solution was cooled and the product precipitated by addition of diethyl ether (25 mL) and collected after chilling for several hours, washing thoroughly with ether. Yield was 0.40 g (91%) of white, partly crystalline solid, which softened at 120 °C and melted at 150 °C: ^1H NMR δ 4.16 (s, 8 H, NCH_2), 4.34 (s, 4 H, OCH_2), 6.7–7.0 (m, 8 H, aromatic); IR (Nujol) cm^{-1} (1775 (s), 1830 (m), cyclic COOCO.

Preparation of BAPTA Monoesters. The general method for making monoesters of BAPTA is illustrated by the synthesis of the bis(4,5-dimethoxy-2-nitrophenyl)methyl ester of BAPTA, **1a**.

BAPTA anhydride (17.6 mg, 40 μmol) and bis(4,5-dimethoxy-2-nitrophenyl)methanol (24 mg, 60 μmol) (prepared by the $NaBH_4$ reduction of the corresponding benzophenone[33]) were heated overnight in dry *N*-methylpyrrolidinone (0.2 mL) at 70 °C. The cooled reaction mixture was treated with saturated aqueous $NaHCO_3$ solution until all effervescence had ceased, diluted with H_2O to ~1 mL, and extracted with CH_2Cl_2 (3 × 0.5 mL) to remove unreacted benzhydrol. The product was precipitated as a pale yellow solid from the aqueous phase on acidification with 4 M hydrochloric acid. Filtration, washing with H_2O, and desiccation yielded 15 mg of monoester **1a** (44%).

RPTLC (Whatman) indicated only a trace of unesterified BAPTA and no diester (solvent system, 70% aqueous MeOH saturated with KH_2PO_4).

Similarly, BAPTA anhydride was reacted with 2-nitro-4,5-dimethoxybenzyl alcohol, 6-nitropiperonal cyanohydrin,[34] 3-nitro-4-quinolinemethanol [prepared by careful saponification of the acetate obtained by reaction of silver acetate in CH_3CN for 3 days at room temperature with 3-nitro-4-(bromomethyl)quinoline[35]] and 8-azido-4-methoxynaphthalenemethanol[16] to yield **1b–1e**, respectively. 4-(Dimethylamino)pyridine catalysis was used with **1c–1e**. All products were essentially free of BAPTA although some had traces of the diester as shown by RPTLC.

Preparation of BAPTA Monoamides. 5,7-Dinitroindoline[36a,b] and 6,8-dinitro-1,2,3,4-tetrahydroquinoline (prepared by dinitration of *N*-acetyl-1,2,3,4-tetrahydroquinoline and deacetylation analogous to 5,7-dinitroindoline) were unreacted with BAPTA anhydride, so instead they were bromoacetylated (using the method described for acetylation[37]) and reacted with 1 equiv of 1,2-bis(2-amino-5-methylphenoxy)ethane,[11] followed by exhaustive alkylation with *tert*-butyl bromoacetate. Ester cleavage by BF_3–HOAc[9a] followed by acid precipitation afforded the BAPTA monoamide free acids **1f** (5,7-dinitroindoline) and **1g** (6,8-dinitro-1,2,3,4-tetrahydroquinoline) essentially pure, as determined by RPTLC.

Quinone Tetraethyl Ester (2e). BAPTA phenol (prepared by catalytic hydrogenolysis of compound XXIV of Grynkiewicz et al.[26] using the method for compound XXV[26] in the same paper) (0.33 mmol, 200 mg) dissolved in acetone (10 mL) was added in one portion to a solution of potassium nitrosodisulfonate (Fremy's salt)[38] (1.67 mmol, 0.45 g) in aqueous KH_2PO_4 (40 mM, 25 mL) at room temperature. The mixture became cloudy and changed to a red color, producing a red precipitate in 10 min. After 1 h, the acetone was evaporated and the reaction mixture saturated with NaCl, extracted with $CHCl_3$ (3 × 20 mL), dried (Na_2SO_4), and evaporated to dryness. Recrystallization from EtOH afforded the quinone, **2e**: yield 146 mg (73%); mp 125–126 °C; ^1H NMR δ 1.05–1.30 (2 t, 12 H, CH_2CH_3), 2.25 (s, 3 H, $ArCH_3$), 3.9–4.3 (m, 20 H, CH_2) 5.40, 5.70 (2 s, 2 H, quinone H), 6.5–6.75 (m, 3 H, aromatic).

Diazo-1A/1B Tetraethyl Ester (2f,g). Tosyl hydrazide (~20 mg, ~0.1 mmol) was added to a solution of **2e** (30 mg, ~0.05 mmol) in $CHCl_3$ (5 mL) and kept overnight at 4 °C. After evaporation of the

(32) Tanigaki, K.; Ebbesen, T. W. *J. Am. Chem. Soc.* **1987**, *109*, 5883–5884.

(33) Lawson, W.; Perkin, W. H.; Robinson, R. *J. Chem. Soc.* **1924**, *125*, 626–657.

(34) Robinson, G. M.; Robinson, R. *J. Chem. Soc.* **1914**, *105*, 1456–1469.

(35) Baumgarten, H. E.; Barkley, R. P.; Chui, S.-H. L.; Thompson, R. D. *J. Heterocycl. Chem.* **1981**, *18*, 925–928.

(36) (a) Noland, W. E.; Rush, K. R. *J. Org. Chem.* **1964**, *29*, 947–948. (b) Terent'ev, A. P.; Preobrazhenskaya, M. N.; Bobkov, A. S.; Sorokina, G. M. *J. Gen. Chem. U.S.S.R.* (*Engl. Transl.*) **1959**, *29*, 2504–2512.

(37) Gall, W. B.; Astill, D.; Boekelheide, V. *J. Org. Chem.* **1955**, *20*, 1538–1544.

(38) Moser, W.; Howie, R. A. *J. Chem. Soc. A* **1968**, 3039–3043.

solvent, the residue was dissolved in ethyl acetate (2 mL) and triethylamine (0.1 mL) and separated by SiO_2 chromatography, eluting with ethyl acetate containing 1% (v/v) triethylamine. The products solidified on trituration with MeOH as an orange powder. Yield, 19 mg. Chromatography on SiO_2 with 0–2% MeOH–$CHCl_3$ (v/v) as eluent separated the two isomers, diazo-1A and diazo-1B (tetraethyl esters **2f** and **2g**, respectively), with the latter eluting first. Diazo-1B: ^1H NMR ($CDCl_3$) δ 1.05–1.30 (2 t, 12 H, CH_2CH_3), 2.2 (s, 3 H, Ar CH_3), 3.9–4.3 (m, 20 H, CH_2), 5.67, 6.34 (2 s, 2 H, quinone), 6.6–6.85 (m, 3 H, aromatic). Diazo-1A: ^1H NMR was similar except the quinone protons had δ 6.01, 6.52.

Synthesis of Diazo-2, 3-Acetoxy-4-nitrobenzoic Acid (3d). 3-Hydroxy-4-nitrobenzoic acid (Aldrich, 95%; 4.82 g, 25 mmol) was suspended in pyridine (2 mL) and acetic anhydride (20 mL) and heated at 100 °C for 30 min. After being cooled, the mixture was evaporated to near dryness to give a yellow solid, which was suspended in H_2O (40 mL). The solid dissolved slowly and the temperature rose to 50–60 °C to give a clear solution, which on cooling yielded the product, **3d**, as a crystalline yellow solid which was collected by filtration, washed with H_2O, and dried: yield 3.72 g; mp 182–184 °C. The mother liquor, on acidification to pH 1 with concentrated hydrochloric acid, gave a further crop (1.58 g) of slightly impure **3d**, as shown by TLC (silica; butanol–acetic acid–water, 4:1:1, v/v): yield 94%; ^1H NMR ($CDCl_3$, CD_3OD) δ 2.36 (s, 3 H, CH_3), 4.50 (s, OH), 7.90 (s, 1 H, H-2), 8.08 (2 s, 2 H, H-5, H-6). Anal. Calcd for $C_9H_7NO_6$: C, 48.01; H, 3.13; N, 6.22. Found: C, 48.13; H, 3.22; N, 6.12.

***tert*-Butyl 3-Hydroxy-4-nitrobenzoate (3e).** Compound **3d** (2.0 g, 8.9 mmol) was heated at reflux with $SOCl_2$ (6 mL) and DMF (1 drop) until all the solid had dissolved (10 min) and there was no further gas evolution (5 min). The solution was cooled and evaporated to dryness to yield a yellow solid, which was treated with dry *tert*-butyl alcohol (3 mL, 32 mmol) and dry pyridine (4 mL, 49 mmol) in $CHCl_3$ (5 mL) at 0 °C under an Ar atmosphere. After the addition, the mixture was refluxed overnight, cooled, and evaporated to dryness, and then dissolved in hot MeOH (30 mL). Concentrated aqueous KOH (45% w/v) was added dropwise with stirring until a constant pH ~11 was maintained for 30 min, adding portions of H_2O as necessary to dissolve the K^+ salt. The excess alkali was neutralized with a few drops of glacial acetic acid and MeOH removed by rotary evaporation to leave an orange solid, which was dissolved in water (30 mL). After filtration, the product **3e** was precipitated by acidification to pH 5 with concentrated hydrochloric acid. Yield, after washing and desiccation, of a pale yellow powder was 0.80 g (38%), which could be recrystallized from ethanol: mp 117–119 °C; ^1H NMR δ 1.60 (s, 9 H, $C(CH_3)_3$), 7.50 (dd, 1 H, J = 2.5, 9 Hz, H-6), 7.80 (d, 1 H, J = 2.5 Hz, H-2), 8.08 (d, 1 H, J = 9 Hz, H-5). Anal. Calcd for $C_{11}H_{13}NO_5$: C, 55.23; H, 5.48; N, 5.86. Found: C, 55.24; H, 5.34; N, 5.79. When the aqueous filtrate was acidified to pH 2, 3-hydroxy-4-nitrobenzoic acid (0.89 g) was recovered (55%).

1-[5-(*tert*-Butoxycarbonyl)-2-nitrophenoxy]-2-(5-methyl-2-nitrophenoxy)ethane (3f). A mixture of **3e** (239 mg, 1 mmol), 1-bromo-2-(5-methyl-2-nitrophenoxy)ethane[26] (286 mg, 1.1 mmol), and K_2CO_3 (83 mg, 0.6 mmol) in dry *N*-methylpyrrolidinone (0.75 mL) was heated at 140 °C for 10 min with protection from moisture and cooled, and H_2O was added dropwise to precipitate the product (**3f**). After filtration, recrystallization from EtOH gave a white solid: mp 113–114 °C; yield 383 mg (92%); ^1H NMR δ 1.60 (s, 9 H, $C(CH_3)_3$), 2.38 (s, 3 H, Ar CH_3), 4.48 (s, 4 H, CH_2CH_2), 6.7–6.9, 7.6–7.7 (2 m, 6 H, aromatic). Anal. Calcd for $C_{20}H_{22}N_2O_8$: C, 57.41; H, 5.30; N, 6.70. Found: C, 57.59; H, 5.27; N, 6.71.

1-[2-Amino-5-(*tert*-butoxycarbonyl)phenoxy]-2-(2-amino-5-methylphenoxy)ethane (3g). Compound **3f** (264 mg, 0.63 mmol) was catalytically hydrogenated at room temperature and pressure with 50 mg of 5% Pd/C in ethyl acetate–EtOH (1:1). Uptake was complete within 1 h; the reaction mixture was filtered and evaporated to dryness to yield the product, **3g**. Recrystallization from EtOH gave shining colorless plates: mp 154–156 °C; yield 184 mg (81%); ^1H NMR δ 1.60 (s, 9 H, $C(CH_3)_3$), 2.20 (s, 3 H, Ar CH_3), 4.37 (s, 4 H, CH_2CH_2), 6.53–6.8, 7.4–7.6 (2 m, 6 H, aromatic). Anal. Calcd for $C_{20}H_{26}N_2O_4$: C, 67.01; H, 7.31; N, 7.82. Found: C, 67.01; H, 7.34; N, 7.92.

1-[2-[Bis[(methoxycarbonyl)methyl]amino]-5-(*tert*-butoxycarbonyl)-phenoxy]-2-[2-[bis(methoxycarbonyl)methyl]amino]-5-methylphenoxy]-ethane (3h). A mixture of **3g** (143 mg, 0.4 mmol), 1,8-bis(dimethylamino)naphthalene (Proton Sponge) (0.69 g, 0.32 mmol), and methyl bromoacetate (0.3 mL, 0.32 mmol) was heated at 125 °C overnight under N_2. An additional 0.16 mmol each of Proton Sponge and methyl bromoacetate was added and heating continued for 48 h. The reaction mixture was diluted with toluene (20 mL), filtered, and washed with 1 M phosphate buffer, pH 2 (3 × 5 mL) and H_2O (1 × 5 mL). After drying over Na_2SO_4, and evaporation to dryness, trituration with EtOH yielded the product, **3h**. Recrystallization from EtOH gave 203 mg of white solid (78%): mp 98–101 °C; ^1H NMR δ 1.58 (s, 9 H, $C(CH_3)_3$), 2.23 (s, 3 H, Ar CH_3), 3.53 (s, 12 H, OCH_3), 4.09, 4.17, 4.26 (3 s, 12 H, CH_2) 6.6–6.8, 7.4–7.5 (2 m, 6 H, aromatic). Anal. Calcd for $C_{32}H_{42}N_2O_{12}$: C, 59.43; H, 6.55; N, 4.33. Found: C, 59.07; H, 6.42; N, 4.36.

Diazo-2 Tetramethyl Ester: 1-[2-[Bis[(methoxycarbonyl)methyl]-amino]-5-(diazoacetyl)phenoxy]-2-[2-[bis(methoxycarbonyl)methyl]-amino]-5-methylphenoxy]ethane (3j). Compound **3h** (100 mg, 0.15 mmol), was dissolved in 20% CF_3COOH/CH_2Cl_2 (v/v, 2.5 mL) and kept at room temperature overnight. TLC (SiO_2; hexane–ethyl acetate–acetic acid, 29:29:1, v/v) revealed that removal of the *tert*-butyl groups was complete. After dilution with $CHCl_3$ (10 mL), the reaction mixture was washed with saturated $NaHCO_3$ solution, dried over Na_2SO_4, and evaporated to dryness to yield the crude benzoic acid derivative as a colorless foam. The crude acid was dissolved in CH_2Cl_2 (2 mL) and oxalyl chloride (100 μl, 1.1 mmol) and refluxed gently for 10 min before being evaporated to dryness to give the crude acid chloride **3i**. This was used without further purification and was dissolved in CH_2Cl_2 (~0.5 mL), and an excess of ethereal alcohol-free diazomethane solution (~10 mmol, prepared from Diazald in 2-ethoxyethanol) was added at 0 °C. After being kept overnight at room temperature, the reaction mixture was evaporated to dryness to yield the crude product **3j** as a part-crystalline solid, which was purified by SiO_2 chromatography eluting with ethyl acetate–hexane. The resulting yellow oil crystallized on trituration with EtOH and was recrystallized from EtOH to give **3j** as lemon-colored crystals: mp 105 °C; yield 42.3 mg (46%); ^1H NMR δ 2.23 (s, 3 H, Ar CH_3), 4.10, 4.20, 4.27 (3 s, 12 H, CH_2), 5.80 (s, 1 H, CHN_2) 6.6–6.8, 7.1–7.4 (2 m, 6 H, aromatic). Anal. Calcd for $C_{32}H_{42}N_2O_{12}$: C, 56.67; H, 5.58; N, 9.12. Found: C, 56.39; H, 5.51; N, 9.26.

Synthesis of Diazo-3, 3-Methoxy-4-nitrobenzoic Acid (4b). 3-Hydroxy-4-nitrobenzoic acid (Aldrich 95%; 1.93 g, 10 mmol), K_2CO_3 (4 g), and dimethyl sulfate (3.8 mL, 40 mmol) suspended in dry *N*-methylpyrrolidinone (10 mL) were heated at 100 °C for 1 h under an N_2 atmosphere. After cooling, addition of water precipitated the methyl ester, which was filtered, dissolved in hot MeOH, and saponified by adding 1 M NaOH solution (11 mmol). After 30 min, the reaction mixture was evaporated to dryness, dissolved in H_2O, and acidified to pH 2 with concentrated HCl to yield the product **4b**, which was filtered and desiccated. Yield, 1.88 g (95%).

***tert*-Butyl 3-Methoxy-4-nitrobenzoate (4c).** Compound **4b** (0.79 g, 4 mmol) was refluxed in thionyl chloride (5 mL) for 1 h, cooled, and evaporated to dryness. A solution of dry pyridine (0.81 mL, 10 mmol) and dry *tert*-butyl alcohol (0.95 mL, 10 mmol) in $CHCl_3$ (2 mL) was added and the reaction mixture refluxed 2 h, with protection for moisture. After being kept overnight at room temperature, the mixture was evaporated to dryness, dissolved in $CHCl_3$ (30 mL), washed with dilute hydrochloric acid (3 × 15 mL), dried over Na_2SO_4, and evaporated to dryness to yield the crude product, **4c**, as a yellow solid: yield 0.54 g (53%); ^1H NMR δ 1.60 (s, 9 H, $C(CH_3)_3$), 3.97 (s, 3 H, OCH_3), 7.5–7.8 (m, 3 H, aromatic).

***tert*-Butyl 4-Amino-3-methoxybenzoate (4d).** The crude nitrobenzoate **4c** (0.5 g, ~2 mmol) was catalytically hydrogenated at room temperature and pressure with 50 mL of 5% Pd/C in ethyl acetate–95% aqueous EtOH (1:1). Uptake was complete after 5 h, and after being kept overnight, the reaction mixture was filtered and evaporated to dryness to yield the product, **4d**, as a colorless oil, which crystallized on trituration with MeOH. Recrystallization from 95% aqueous EtOH afforded 295 mg (65%) of white crystals. Anal. Calcd for $C_{12}H_{17}NO_3$: C, 64.55; H, 7.68; N, 6.27. Found: C, 64.46; H, 7.68; N, 6.23.

***tert*-Butyl 4-[Bis[(methoxycarbonyl)methyl]amino]-3-methoxybenzoate (4e).** A mixture of compound **4d** (226 mg, 1 mmol), 1,8-bis(dimethylamino)naphthalene (0.86 g, 4 mmol), and methyl bromoacetate (0.38 mL, 4 mmol) were heated at 125 °C under Ar for 96 h, with a further addition of 2 mmol each of 1,8-bis(dimethylamino)naphthalene and methyl bromoacetate after 24 h. After cooling, the reaction mixture was diluted with ethyl acetate–toluene (1:1, 30 mL), filtered, and washed with 1 M phosphate buffer pH 2 (3 × 10 mL) and then H_2O (1 × 10 mL). The organic layer was dried (Na_2SO_4) and evaporated to dryness to yield an oil, which was chromatographed on SiO_2 with ethyl acetate–hexane as eluant to yield **4e** as a colorless oil (175 mg, 47%): ^1H NMR δ 1.53 (s, 9 H, $C(CH_3)_3$), 3.73 (s, 6 H, CO_2CH_3), 3.80 (s, 3 H, Ar OCH_3), 4.15 (s, 4 H, CH_2), 6.68 (d, 1 H, J = 8 Hz, H-5), 7.43 (s, 1 H, H-2), 7.48 (d, 1 H, J = 8 Hz, H-6).

Diazo-3 Dimethyl Ester: *tert*-Butyl 4-[Bis[(methoxycarbonyl)-methyl]amino]-2′-diazo-3-methoxyacetophenone (4f). The free acid was prepared by dissolving the ester **4e** (90 mg, 0.24 mmol) in 20% CF_3COOH/CH_2Cl_2 (2.5 mL, v/v) and keeping at room temperature overnight. The reaction mixture was diluted with CH_2Cl_2, extracted into saturated aqueous $NaHCO_3$ (1 × 15 mL), acidified with glacial acetic acid and reextracted (6 × 10 mL) with $CHCl_3$. After the organic layer

(Na_2SO_4) was dried, evaporation of the solvent yielded the crude free acid as a white solid, yield 66 mg (87%). The crude product was dissolved in CH_2Cl_2 (3 mL), oxalyl chloride (100 μL, 1.1 mmol) added dropwise, and the resultant mixture refluxed gently for 10 min. The crude acid chloride, after evaporation of the reaction mixture, was used without further purification and was redissolved in $CHCl_3$ (2 mL); the resultant mixture was added to an excess of ethereal alcohol-free diazomethane solution (~10 mmol) at 0 °C. The solution was allowed to warm up to room temperature over 2 h and then kept overnight. Evaporation of the solvent yielded the crude product, which was separated by SiO_2 chromatography with ethyl acetate–hexane: yield of pale yellow oil, 64 mg (80%); ^1H NMR 3.73 (s, 6 H, CO_2CH_3), 3.80 (s, 3 H, Ar OCH_3), 4.15 (s, 4 H, CH_2), 5.78 (s, 1 H, CHN_2), 6.62 (d, 1 H, J = 8 Hz, H-5), 7.10 (dd, 1 H, J = 2, 8 Hz, H-6), 7.33 (d, 1 H, J = 2 Hz, H-2).

Synthesis of Diazo-4. 1,2-Bis[5-(*tert*-butoxycarbonyl)2-nitrophenoxy]ethane (5b). A mixture of compound **3e** (0.24 g, 1 mmol) and K_2CO_3 (0.14 g, 1 mmol) in *N*-methylpyrrolidone (1 mL) was heated at 125 °C under Ar. After all gas evolution had ceased (5 min), 1,2-dibromoethane (total 102 μL, 1.2 mmol) was added in three equal portions at 5, 20, and 35 min. The mixture was then heated for 15 min and cooled, and H_2O was added dropwise to precipitate the crude product as a white solid, which was collected by filtration and washed thoroughly with H_2O. Recrystallization from EtOH afforded compound **5b** as brown crystals (0.21 g, 83%): mp 155–157 °C; ^1H NMR δ 1.60 (s, 18 H, $C(CH_3)_3$), 4.53 (s, 4 H, CH_2), 7.5–7.8 (m, 6 H, aromatic). Anal. Calcd for $C_{24}H_{28}N_2O_{10}$: C, 57.14; H, 5.59; N, 5.55. Found: C, 56.81; H, 5.50; N, 5.78.

1,2-Bis[(2-amino-5-(*tert*-butoxycarbonyl)phenoxy]ethane (5c). Compound **5b** (0.42 g, 0.83 mmol) was dissolved in ethyl acetate–ethanol (45 mL, 2:1) and catalytically hydrogenated at room temperature and pressure with 100 mg of 5% Pd/C. Uptake was complete within 1 h. The reaction mixture was filtered and evaporated to dryness to yield the product **5c**. Recrystallization from EtOH gave a white powder (two crops, total 0.35 g, 95%): mp 138 °C; ^1H NMR δ 1.58 (s, 18 H, $C(CH_3)_3$), 4.20 (s, br, 4 H, NH_2), 4.40 (s, 4 H, CH_2), 6.60 (d, 2 H, H-3), 7.45 (m, 4 H, H-4,6). Anal. Calcd for $C_{24}H_{32}N_2O_6$: C, 64.84; H, 7.26; N, 6.30. Found: C, 64.61; H, 7.33; N, 6.74.

1,2-Bis[2-[bis[(methoxycarbonyl)methyl]amino]-5-(*tert*-butoxycarbonyl)phenoxy]ethane (5d). A mixture of compound **5c** (185 mg, 0.42 mmol), 1,8-bis(dimethylamino)naphthalene (0.86 mg, 4 mmol), and methyl bromoacetate (0.38 mL, 4 mmol) was heated for 5 days at 125 °C under Ar. The resulting solid was dissolved with ethyl acetate–chloroform (20 mL), filtered, and washed with 1 M phosphate buffer, pH 2 (1 × 5 mL), and H_2O (1 × 5 mL). After drying over Na_2SO_4, and evaporation to dryness, the resulting solid was recrystallized from EtOH to give the product, **5d**, as a white solid (0.23 g, 64%): mp 144–145 °C; ^1H NMR δ 1.54 (s, 18 H, $C(CH_3)_3$), 3.57 (s, 12 H, OCH_3), 4.17 (s, 8 H, NCH_2), 4.28 (s, 4 H, OCH_2), 6.69 (d, 2 H, J = 9 Hz, H-3), 7.48 (s, 2 H, H-6), 7.52 (d, 2 H, J = 9 Hz, H-4). Anal. Calcd for $C_{36}H_{48}N_2O_{14}$: C, 59.00; H, 6.60; N, 3.82. Found: C, 58.77; H, 6.46; N, 3.80.

Diazo-4 Tetramethyl Ester: 1,2-Bis[2-[bis[(methoxycarbonyl)methyl]amino]-5-(diazoacetyl)phenoxy]ethane (5e). Compound **5d** (100 mg, 0.11 mmol) was dissolved in 20% CF_3COOH/CH_2Cl_2 (v/v, 2.5 mL), kept at room temperature overnight, and then evaporated to dryness. The resulting crude diacid was suspended in CH_2Cl_2 (2 mL) containing 1 drop of dry DMF; oxalyl chloride (0.5 mL, 5.7 mmol) was added and the mixture refluxed for 15 min. The resulting yellow solution of crude diacid chloride was evaporated to dryness, redissolved in CH_2Cl_2 (2 mL), and treated with an excess of ethereal, alcohol-free diazomethane at 0 °C. After standing overnight at room temperature, the solution was evaporated to dryness and the product, **5e**, was separated by SiO_2 chromatography with ethyl acetate–hexane as eluent. Recrystallization from EtOH gave **5e** as a pale yellow solid (31 mg, 42%): mp 151 °C dec; ^1H NMR δ 3.58 (s, 12 H, OCH_3), 4.18 (s, 8 H, NCH_2), 4.28 (s, 4 H, OCH_2), 5.81 (s, 2 H, CHN_2), 6.78 (d, 2 H, J = 9 Hz, H-3), 7.20 (dd, 2 H, J = 2.5, 9 Hz, H-4), 7.42 (d, 2 H, J = 2.5 Hz, H-6). Anal. Calcd for $C_{30}H_{32}N_6O_{12}$: C, 53.89; H, 4.82; N, 12.57. Found: C, 53.89; H, 4.92; N, 12.39.

Saponification of Esters. Diazo-2 tetramethyl ester was saponified to the tetraanion by dissolution in MeOH (gentle heat), addition of an excess of aqueous 1 M KOH solution, and keeping at room temperature several hours, preferably overnight. Diazo-2 is stable under such conditions of dilute aqueous base but on concentration to a solid decomposes and becomes light-insensitive. The purity of diazo-2 solutions can be determined by measuring the extent of absorbance change on complete photolysis (Figure 1B) as contaminants contribute absorbance at 355 nm. Diazo-1, -3, and -4 esters were saponified analogously.

Preparation and Acetoxymethyl (AM) Esters. Diazo-2 tetramethyl ester **3j** (2.0 mg) was dissolved in MeOH (100 μL) and saponified by the addition of tetramethylammonium hydroxide (40 μL, 1 M aqueous solution). After the mixture was kept at room temperature overnight, glacial HOAc (2.3 μL, 40 μmol) was added and the solution evaporated to dryness (waterbath <30 °C) and desiccated. The residue was suspended in CH_2Cl_2 (0.5 mL), and then diisopropylethylamine (5 μL) and acetoxymethyl bromide[26] (10 μL) were added with stirring. After 6 h, an additional 10 μL each of amine and bromide was added and the mixture stirred overnight at room temperature. The reaction mixture was diluted with $CHCl_3$ (1 mL) and extracted with 50 mM phosphate buffer, pH 6.8 (1 × 1 mL), dried over Na_2SO_4, evaporated to dryness, and separated by SiO_2 chromatography, eluting with ethyl acetate–hexane to afford diazo-2/AM as a colorless gum. Stock solutions were prepared in DMSO and stored frozen. Diazo-3/AM and -4/AM esters were prepared similarly.

Calcium and Magnesium Affinities. Ca^{2+}-binding constants for chelators before and after photolysis were determined by monitoring UV spectra during titration of EGTA or HEEDTA buffers to varying free Ca^{2+} levels.[4a,b] Either the ratio of, for example, [Ca·EGTA] to free [EGTA] was adjusted at a constant pH or the pH was varied while [Ca·EGTA] = [EGTA]. These two approaches gave equivalent answers for pH >7 whenever directly tested, thanks to the pH insensitivity of BAPTA-like ligands[11] (see Figure 1 legend for more details). The apparent dissociation constants of Ca·EGTA and Ca·HEEDTA were calculated as described elsewhere.[4a,26,39]

Free [Mg^{2+}] was likewise controlled by Mg EGTA buffers, assuming an apparent dissociation constant for the Mg·EGTA complex (including its monoprotonated form) of 6 mM at pH 7.60 in 0.1 M ionic strength.[4a,39]

Quantum Efficiencies of Photolysis. The photolysis quantum efficiencies of BAPTA monoesters and monoamides as well as the diazo chelators were determined by alternately irradiating a buffered solution of the substrate with a known intensity of long-wavelength UV light (365 nm) and measuring the absorbance spectrum, in apparatus previously described.[4b] The quantum efficiencies of nitrobenzyl models were measured by monitoring the loss of starting material (and formation of product, where possible), following separation by HPLC (Waters Associates, Inc., Milford, MA) on a Supelcosil LC-18 column (Supelco, Inc., Bellefonte, PA) using CH_3CN-H_2O eluant and a UV detector. Quantum efficiencies were calculated as described previously.[4b]

Flash Photolysis. Kinetics of the conversion of diazo-2 and diazo-3 to the carboxylic acid products and the kinetics of Ca^{2+} binding by photolyzed diazo-2 were measured by flash photolysis and pH monitoring. The experiments were done in a Dialog apparatus (Garching, FRG) normally used for temperature jumps. The xenon flash lamp was a Model 6100SP7 (Photochemical Research Associates, London, Ontario, Canada) modified to give a light pulse with a full width at half-maximum of 85 μs. The output of the xenon lamp was passed through a UG-2 filter to yield broad-band UV radiation in the 330–390-nm range. Since neither the flash lamp nor the kinetic spectrometer was optimized for light energy, the response amplitudes achieved in the experiments are far from those attainable during a biological experiment.

The cresol red used for reporting pH changes in the sample solutions was probed with 572-nm light from a 200-W Hg–Xe arc lamp and a grating monochromator. Glass filters blocking wavelengths shorter than 455 and 530 nm were placed in front of the reference and signal photomultipliers, respectively, to minimize stray light from the photolytic flash fron entering the detector. Despite these precautions, some flash artifact still occurred, as evidenced by the initial spikes in the records shown in Figure 2. The transmitted 572-nm light signal was digitized by a Biomation 805 (Biomation, Cupertino, CA) transient wave-form recorder triggered by a sync pulse generated by the xenon flash lamp power supply. The digitized data were transferred via a PET microcomputer (Commodore Business Machines, Santa Clara, CA) to a VAX 11/785 minicomputer where all data reduction and analyses were performed. The program DISCRETE[40a,b] was used to analyze the data for multiple-exponential decay times.

Experiments to determine the rate of photochemical product formation from diazo-2 were made at low free Ca^{2+} (either no added Ca^{2+} or in the presence of 40 μM BAPTA) and high free Ca^{2+} (1 mM $CaCl_2$). Ca^{2+} binding kinetics of the photolyzed diazo-2 was studied with samples that contained 70 μM diazo-2, 2.0 mM K_2H·HEEDTA, and 1.0 mM $CaCl_2$. For the diazo-3 experiments, the samples contained either 35 or 70 μM diazo-3. All solutions contained 100 mM KCl as background electrolyte and enough cresol red to yield a maximum absorbance of 0.07 in the sample cell. The measurements were made at 20 °C and pH 8.0, ad-

(39) Martell, A. E.; Smith, R. M. *Critical Stability Constants*; Plenum: New York, 1974; Vol. 1.

(40) (a) Provencher, S. W. *Biophys. J.* **1976**, *16*, 27–41. (b) Provencher, S. W. *J. Chem. Phys.* **1976**, *64*, 2772–2777.

justed with KOH under helium purge before the solution was sealed into the sample cell.

Control flashes delivered to solutions containing cresol red but from which diazo compound was omitted (Figure 2A, dotted trace) showed that flash duration and detector recovery did not limit time resolution.

In Vivo Biological Tests. For preliminary biological tests, Fisher rat embryo fibroblasts of the REF52 cell line were cultured as previously described.[9b] For testing diazo-2, REF52 cells were incubated for 30 min at 25 °C in Dulbecco's modified Eagle's medium (DMEM), buffered at pH 7.4 with 20 mM HEPES and containing 1 μM diazo-2/AM and 10 μM fluo-3/AM. For control experiments using diazo-3, the cells were incubated for 90 min at 25 °C in DMEM, buffered to pH 7.4 with 20 mM HEPES and containing 1 μM diazo-3/AM and 10 μM fluo-3/AM. After loading, the cells were gently washed, transferred into Hanks' balanced salt solution containing 0.2 mM sulfinpyrazone to inhibit nonspecific organic anion transport,[41] and mounted on a 25 °C microscope stage for experimentation.

Flash photolysis of trapped cellular diazo-2 and the concomitant monitoring of intracellular free Ca^{2+} concentration with fluo-3, a fluorescent Ca^{2+} indicator,[9a] were performed by methodology and instrumentation developed previously.[9b] Briefly, output from a Xe arc lamp was passed through a monochromator to yield the 490-nm light used to probe the fluo-3 trapped intracellularly. The fluo-3 fluorescence images of the cells were recorded with a silicon-intensified target camera. Images were stored on a high-resolution monochrome laser disc recorder (Panasonic TQ-2028) for delayed processing. Photolyses were performed by briefly moving a chopper mirror to send broad-band UV from an XBO 75-W xenon arc lamp and a UG-2 filter into the microscope instead of 490-nm fluo-3 excitation. The microscope objective (Nikon UV-CF, 40X) was chosen for its high UV transmission and numerical aperture (1.3). A custom dichroic mirror (DR505LP, Omega Optical, Inc., Brattleboro, VT) was placed in the microscope epifluorescence filter cube to reflect both UV and 490-nm light efficiently while retaining high transmission at wavelengths greater than 510 nm, where fluo-3 emits strongly. Data acquisition by the camera and the flash photolysis were under the coordinated control of a Micro-PDP-11/73 computer. The same computer was used to analyze the fluorescence images acquired during the experiment.

Covalent Modification of Lysine by Photochemical Intermediates. To study the extent to which biological substrates may be covalently modified by reactive intermediates generated by the photolysis of the diazoketones, we photolyzed 100 μM diazo-3 in the presence of 10 mM phosphate and either 100 mM KCl or 100 mM lysine hydrochloride, at pH 7.2. The photolysates were analyzed by HPLC (Waters Associates, Inc., Milford, MA; C-18 column, Supelco, Inc., Bellefonte, PA), with 10 mM KH_2PO_4/K_2HPO_4 buffer at pH 7.2 as eluting solvent. The absorbance of the eluate at 254 nm was monitored. Before being injected onto the column, concentrated stock solutions of either KCl or lysine hydrochloride were added to the photolysate to ensure that the electrolyte compositions of the injected samples were identical. Thus, 10 μL of 1 M KCl was added to 100 μL of the sample of diazo-3 photolyzed in lysine hydrochloride, while 10 μL of 1 M lysine hydrochloride was added to 100 μL of the sample of diazo-3 photolyzed in KCl.

Acknowledgment. This work was supported by Grants GM31004 and EY04372 from the National Institutes of Health and Grant 83-K-111 from the Searle Scholars Program to R.Y.T. We thank Prof. I. Tinoco, Jr., of the Department of Chemistry at the University of California, Berkeley, for the use of the rapid kinetics apparatus.

(41) Tsien, R. Y. *Annu. Rev. Neurosci.* **1989**, *12*, 227-253.

The Direct Insertion Mechanism in Ziegler-Natta Polymerization: A Theoretical Study of $Cp_2TiCH_3^+ + C_2H_4 \rightarrow Cp_2TiC_3H_7^+$

Cynthia A. Jolly and Dennis S. Marynick*

Contribution from the Department of Chemistry, Box 19065, The University of Texas at Arlington, Arlington, Texas 76019-0065. *Received November 16, 1988*

Abstract: The direct insertion mechanism for the polymerization of ethylene using a real Ziegler-Natta initiator has been studied using PRDDO and ab initio electronic structure calculations. Geometries were optimized at the PRDDO level and energetics were reevaluated at the ab initio Hartree-Fock level with and without MP2 corrections. The calculated barrier for the direct insertion reaction $Cp_2TiCH_3^+ + C_2H_4 \rightarrow Cp_2TiC_3H_7^+$ is +9.8 kcal/mol at the MP2 level. This is in excellent agreement with the experimental barrier of 6-12 kcal/mol. The calculated ΔE for the overall reaction is -12.4 kcal/mol. The geometries of several structures along the reaction pathway including the transition state are presented. The structure of the transition state was found to resemble a metallocyclobutane ring as is generally assumed for the direct insertion mechanism. Localized molecular orbitals are employed to qualitatively analyze the bonding in these complexes. A comparison of our results with similar calculations on the model system $Cl_2TiCH_3^+ + C_2H_4 \rightarrow Cl_2TiC_3H_7^+$ is also presented.

The insertion of olefins into transition-metal alkyl bonds is the fundamental process in Ziegler-Natta polymerization. Yet, despite more than 30 years of study, the mechanism of polymerization is still not fully understood. Several schemes[1] have been proposed for the olefin insertion step; however, experimental results have not definitely proven any one mechanism. The problem in determining the mechanism arises from the fact that most of the Ziegler-Natta initiators are heterogeneous, making them very difficult to study quantitatively. Three basic mechanisms have been proposed. The first and most widely accepted mechanism is the direct four-center olefin insertion mechanism suggested by Cossee and Arlman (Figure 1).[1a-c] The transition state in this scheme may be loosely described as a metallocyclobutane ring-type complex. In some variations on this mechanism, an alkyl-aluminum species is also involved in the mechanistic details; however, in the simplest version of this mechanism the alkyl-aluminum species is required only to alkylate a transition-metal complex, thus forming an active initiator. Second, a metathesis-type mechanism has been proposed by Green and Rooney (Figure 2).[1e,f] In this scheme, there is an α-hydrogen shift from the growing

(1) (a) Cossee, P. *J. Catal.* **1964**, *3*, 80. (b) Arlman, E. J. *J. Catal.* **1964**, *3*, 89. (c) Arlman, E. J.; Cossee, P. *J. Catal.* **1964**, *3*, 99. (d) McKinney, R. J. *J. Chem. Soc., Chem. Commun.* **1980**, 491. (e) Ivin, K. J.; Rooney, J. J.; Stewart, C. D.; Green, M. L. H.; Mahtab, R. *J. Chem. Soc., Chem. Commun.* **1978**, 604. (f) Green, M. L. H. *Pure Appl. Chem.* **1978**, *50*, 27. (g) Pino, P.; Mulhaupt, R. *Angew. Chem., Int. Ed. Engl.* **1980**, *19*, 857.

0002-7863/89/1511-7968$01.50/0